Desalination and Water Treatment
www.deswater.com

doi: 10.5004/dwt.2022.28185

250 (2022) 80–99
February

Developing bioadsorbents from orange peel waste for treatment of raw textile industry wastewater

Santiago Bedoya Betancur[a], Sebastian Amar Gil[a], Alba N. Ardila A.[a,*], Erasmo Arriola V.[a], Rolando Barrera Z.[b], José A. Hernández[c], T.A. Zepeda[d]

[a]*Research Group in Environmental Catalysis and Renewable Energies, Facultad de Ciencias Básicas Sociales y Humanas, Politécnico Colombiano Jaime Isaza Cadavid, Apartado Aéreo 49-32, Medellín, Colombia, emails: anardila@elpoli.edu.co (A.N. Ardila A.), santiago_bedoya27081@elpoli.edu.co (S.B. Betancur), sebastianamar@elpoli.edu.co (S. Amar Gil), erasmoarriola@elpoli.edu.co (E. Arriola V.)*
[b]*Grupo CERES Agroindustria e Ingeniería, Facultad de Ingeniería, Universidad de Antioquia UdeA, Calle 70 No. 52-21, Medellín, Colombia, email: rolando.barrera@udea.edu.co*
[c]*Instituto Politécnico Nacional UPIIG. Av. Mineral de Valenciana 200, Col. Fraccionamiento Industrial Puerto Interior, 36275 Silao de la Victoria, Gto., México, email: jahernandezma@ipn.mx*
[d]*Centro de Nanociencias y Nanotecnología, Universidad Nacional Autónoma de México, Ensenada, BC. 22800, México, email: trino@cnyn.unam.mx*

Received 14 August 2021; Accepted 16 January 2022

ABSTRACT

In this study, two bioadsorbents were developed by the pyrolysis from orange peel waste at 500°C and 700°C, respectively. Both biochars were characterized and evaluated for the treatment of a real raw textile industry wastewater from Medellin-Colombia. Additionally, the pollutant removal efficiency of synthesized biochars was compared with a commercial activated carbon (CAC). Synthetized materials showed no important variations between them in terms of chemical composition, morphology, structure, and textural properties. The maximum removal percentages for color, chemical oxygen demand, biochemical oxygen demand and total organic carbon were found be 32%, 30%, 68% and 52%, respectively, for the biochar obtained at 700°C under optimal conditions (100 mg of biochar at 25°C and pH of 3.0). The removal percentages for the same parameters under similar adsorption conditions were 22%, 15%, 14% and 27%, respectively, using the CAC. It is noticed that all values are smaller than those achieved with the bioadsorbents produced in this study. Thus, bioadsorbents from orange peel waste could be an alternative low-cost material for treatment of real raw textile industry wastewater.

Keywords: Orange peel waste; Bioadsorbent; Textile industry wastewater; Adsorption process

1. Introduction

Textile wastewater contains numerous toxic substances including dyes type azo, anthraquinone and phthalocyanine; as well as different organic compounds and heavy metals [1–3]. In the textile industry several reactive dyes are extensively used, which remain in the dye bath after the dying process, making colored effluent, due to the presence of chromophore groups in their structure [4–6]. Additionally, the textile wastewater usually contains high concentrations of total organic carbon (TOC), biochemical oxygen demand (BOD), chemical oxygen demand (COD), total dissolved solids (TDS) and includes highly alkaline values of pH [1,5,7,8]. Therefore, the discharges of high volumes of textile wastewater into aquatic environment without treatment could be harmful to human health, the

* Corresponding author.

aquatic life (flora and fauna) and may cause alteration of physical, chemical, and biological properties of the lakes, rivers and wetlands [1,3,9].

Many different techniques have been extensively studied for the treatment of textile industrial wastewater, including physicochemical and biological treatments and advanced oxidation processes [7,10–12]. Effectiveness of selected treatment will depend on different parameters, including the wastewater composition, the load and type of contaminants and the process conditions, among others. Different treatment strategies could present limitations, advantages, and disadvantages according to the case study or the particularities of the process [13–15]. Adsorption-based processes are considered one of the most versatile techniques for the wastewater treatment [16]. Such techniques often use activated carbon as adsorbent because its porous structure, high surface area, chemical stability, and adsorption capacity [17,18]. Nonetheless, it has some drawbacks such as high production cost. In addition, it is mainly produced from fossil raw materials like coal, petroleum pitch, and phenolic resin [16,19]. In order to replace the expensive activated carbon, as well as decrease the demand for fossil resources and seek for more environmentally friendly processes, different biochars from natural materials and agro-industrial waste have been also tested and adopted as biosorbents for the elimination of pollutants from wastewater [16,19–22].

The biosorbents generated from lignocellulosic sources play an important role in eliminating toxic substances from wastewater. Citrus waste (i.e., orange peels) are used as biosorbents because they are abundant, cheap and widely available through biomaterials discarded in fresh fruit stalls, juice shops and orange processing industry. Moreover, globally harvest of citrus brings about 100 million tons annually, of which 55%–60% of the give-forth transforms into waste. These agro-industrial waste are commonly disposed at landfill; however, its chemical composition allow to [23,24] addition, the adsorption capacity of these type of adsorbents can be improved through chemical modifications [23,25]. Table 1 summarizes major findings in the literature regarding with the adsorption capacity and removal percentage for various pollutants using bioadsorbents derived from orange peel waste. None of them uses real wastewater. In fact, in most studies ideal solutions or synthetic industrial wastewater with an only pollutant are used; thus, there is still limited information towards the practical application of these adsorbents in real wastewater [26–28]. Using real wastewater matrices in adsorption studies is a challenge due to its complex composition and variation on this kind of effluent [5].

In this study, two biochars from orange peel waste were prepared by pyrolysis at two different temperatures. Their adsorption capability was evaluated through the pollutants removal in a real wastewater from the textile industry. Wastewater and biochars were characterized in order to improve the understanding on the biosorption process. Experimental conditions such as pH, temperature and adsorbent loading were fixed according to previous results (See supporting information) and literature findings. Additionally, the efficiency of the bioadsorbents for color and other pollutants removal from real wastewater were compared with adsorption capability of a commercial activated carbon under similar process conditions. Unlike most related studies in the literature, in this contribution bioadsorption process were carried out using a raw wastewater; therefore, the results are expected to help close technological gaps between research on bioadsorbents and their real application in textile industry.

2. Materials and methods

2.1. Obtention and characterization of biochars

Waste oranges of the *Citrus sinensis* species (fruits that due to their size do not comply with the NTC 4086 standards for their commercialization) were collected from a harvest area at department of Caldas, Colombia. It was peeled, sliced and dried at 105°C during 24 h for removal the moisture contents. Then were grounded using a blade mill. The obtained powders were loaded into a stainless-steel vertical tubular reactor placed in a tube furnace for the pyrolysis from 25°C to 500°C, or from 25°C to 700°C; both cases at 10°C/min and under N_2 constant flow of 25 mL/min. Once the desired pyrolysis temperature was reached, the material was left for 3 h. Materials prepared at 500°C and 700°C were coded POP1 and POP2, respectively. Commercial activated carbon (CAC) type Darco 20 × 40 and produced by Norit (Norit Americas Inc.) was selected for biosorption comparisons with orange peel biosorbents prepared in this study [42].

Crystalline phases were determined from X-ray powder diffraction patterns (XRD) collected in air at room temperature with a Bruker D8 ADVANCE diffractometer (Bragg-Brentano θ-θ geometry, Cu Kα radiation, a Ni 0.5% Cu-Kβ filter in the secondary beam, and a one-dimensional position-sensitive silicon strip detector (Bruker, Lynxeye)). The diffraction intensity was measured in the 15°–70° 2θ range using a 0.02°/min 2θ step rate. Textural properties (surface area, size pore and pore volume) were evaluated by N_2 adsorption–desorption isotherms at 75.2 K using a Micromeritics ASAP 2020. The Brunauer–Emmett–Teller (BET) equation was used for determining the surface area (BET) based on N_2 isotherms. The point of zero charge (pH_{PZC}) of the biochars was determined by the method of mass titration, which involves finding the asymptotic value of the pH of a biochar/water slurry as the biochar mass content is increased. Different amounts of biochar were added to water (typical values of biomaterial/water by weight were 20, 40, 60, 80 and 100 mg) and the resulting pH values were measured after 24 h of equilibration. The pH values of the point of zero charge were estimated from potentiometric titration. Attenuated total reflectance-Fourier transform infrared spectroscopy (ATR-FTIR) analyses were carried out over the wave number range of 4,000–500 cm^{-1} using a Shimadzu IRAffinity-1S. Thermogravimetric analysis (TGA) was carried out on a TGA Q500 TA Instruments at a heating rate of 40°C/min within the range of 30°C–800°C under a nitrogen atmosphere with flow rate of 20 mL/min. Morphology and elemental composition of the biochars were investigated by using a field emission scanning electron microscopy (SEM) in a JSM-5800 F JEOL at 5.0 kV. In addition, carbon, hydrogen, nitrogen, and oxygen content were found out using the CHNS analyzer (Leco TruSpec Micro and 628 O analyzers, USA) using the ASTM D-5373-08 method.

Table 1
Comparison of the adsorption capacity and removal percentage for various pollutants using bioadsorbents derived from orange peel waste

Adsorbent	Adsorbate	Hue type	Removal (%)	Adsorption capacity (mg g^{-1})	Adsorption conditions	References
Orange peel	Crystal violet dye	Synthetic water	86.7	22.7	1,000 mg/L of adsorbent, 60°C, pH > 8 and 50 mg/L of dye.	[26]
Magnetized orange peel waste	Crystal violet dye	Synthetic water	91.1	46.9	1,000 mg/L of adsorbent, 60°C, pH > 8 and 50 mg/L of dye.	[26]
Orange peel (Microwave-assisted pyrolysis <500°C)	Malachite green dye	Synthetic water	–	28.5	20,000 mg/L of adsorbent, room temperature and 1 mg/L of dye.	[29]
Orange peel (Furnace 400°C)	Reactive red dye	Aqueous solution	89.4	1.7	1 g of adsorbent, 30°C, pH of 4, and 25 mg/L of dye.	[30]
Orange peel (Magnetized)	Methylene blue dye	Aqueous solution	91.4	40	1 g of adsorbent, 40°C, pH of 8, and 50 mg/L of dye.	[31]
Orange peel sulfuric acid-treated	Methylene blue dye	Aqueous solution	98.1	50.0	10,000 mg/L of adsorbent, 30°C, pH of 8 and 250 mg/L of dye.	[32]
Orange peel	Reactive gray BF-2R	Aqueous solution	60	11.4	60,000 mg/L of adsorbent, 25°C, pH of 2 and 100 mg/L of dye.	[33]
Activated carbon orange peel (COP)	Violet B	Aqueous solution	70	49.2	100 mg/L of adsorbent, 25°C, pH of 2 and 150 mg/L of dye.	[34]
Orange peel (Modified with quaternary amine)	Reactive red 120 dye	Aqueous solution	91	344.8	50 mg/L of adsorbent, 65°C, pH of 2, and 300 mg/L of dye.	[23]
Orange peel (pyrolysis CO_2 > 800°C)	Congo red dye	Aqueous solution	89.0	91	3,000 mg/L of adsorbent, room temperature, pH of 2–3, and 1,000 mg/L of dye.	[24]
Orange peel (Steam at 700°C)	Congo red dye	Aqueous solution	93.0	136	3,000 mg/L of adsorbent, room temperature, pH of 2–3, and 1,000 mg/L of dye.	[24]
Orange peel (Modified with phosphoric acid)	Methylene blue dye	Aqueous solution	–	307.6	50 mg/L of adsorbent, 25°C, pH of 2–3, and 100 mg/L of dye.	[35]
Orange peel (Cationic modified)	Congo red dye	Aqueous solution	–	163	0.05 g of adsorbent, 45°C, pH of 3, 300 mg/L of dye	[36]
Orange peel (pyrolysis 660°C)	Ni(II)	Aqueous solution	–	17.6	1 g, room temperature, pH of 7.5, 100 mg/L of heavy metal.	[37]
Orange peel (Chemical cross-linking)	Cr(VI)	Aqueous solution	80.4	107.5	4 g of adsorbent, room temperature, pH of 4, 23 mg/L of heavy metal.	[38]
	Cu(II)	Aqueous solution	82.5	116.6	4 g of adsorbent, room temperature, pH of 5, 100 mg/L of heavy metal.	[38]
Orange peel (combustion 400°C)	Cu(II)	Aqueous solution	95.0	16.6	0.5 g of adsorbent, 45°C, pH of 5, 36 mg/L of heavy metal.	[39]
Orange peel (cellulosic waste)	Cu(II)	Aqueous solution	–	63.0	1,000 mg/L of adsorbent, 20°C, pH of 5, 100 mg/L of heavy metal.	[40]
Orange peel	Cd(II)	Aqueous solution	–	160.3	100 mg/L of adsorbent, 25°C, pH of 5, 1,000 mg/L of heavy metal.	[41]

2.2. Sampling and physicochemical characterization of real textile wastewater

Raw real textile industry wastewater was collected on the outskirts of Medellin-Colombia. This wastewater contains textile effluents that include mixture of different dyes and correspond to common plant outlet discarded from conventional textile dyeing processes. To obtain the typical spectral characteristics of textile wastewater, sampling was conducted just after the dyeing process and before entering the company's treated wastewater plant. Samples were manually collected with intervals of 15 min during 3 h in clean polyethylene bottles. Field data for temperature, pH, conductivity, turbidity, true and apparent color were performed in situ. After sampling was completed, a final composite sample of 12 L was obtained by mixing collected samples. The composite wastewater collected was acidified with 2% sulfuric acid to prevent the growth of microorganisms and was stored in the 4°C refrigerator until it was analyzed or treated. Physicochemical parameters like total solids, total settleable solids, total alkalinity, total acidity, total chlorides, total nitrates, and heavy metal contents (Cu, Cr, Cd, Ni, Zn and Co), TOC, COD and BOD_5 were determined ex situ. All sampling and characterization were performed following the Standard Methods of Examination of Water and Wastewater (Table 2) [43].

Table 2
Physicochemical parameters evaluated and applied method

Parameter	Method	TIWW1
Color	Color to naked eye	Blue-Black
True color, Pt-Co	AWWA-2120	550
Temperature, °C	AWWA-4500H$^+$	25
pH	AWWA-4500H$^+$	9.90
Electrical conductivity, μS/cm	AWWA-2510B	169
Turbidity, NTU	AWWA-2130B	69.1
Total solids, mg/L	AWWA-2540B	3,320
Total settleable solids, mg/L	AWWA-2540E	0
Total alkalinity, mg $CaCO_3$/L	AWWA-2320B	1,134.0
Total acidity, mg $CaCO_3$/L	AWWA-2310B	590.6
Total nitrates, mg/L	AWWA-4500B	222.3
Total chlorides, mg/L	AWWA-4500-Cl$^-$ D	1,800
Total copper (Cu), mg/L	AWWA-3500 Cu	0.25
Total chromium (Cr), mg/L	AWWA-3500-Cr B	2.57
Total cadmium (Cd), mg/L	AWWA-3500 Cd	0.02
Total nickel (Ni), mg/L	AWWA-3500 Ni	0.04
Total zinc (Zn), mg/L	AWWA-3500 Zn	3.84
Total cobalt (Co), mg/L	AWWA-3111 Co B	0.250
Total organic carbon (TOC), mg O_2/L	AWWA-5310B	854.6
Chemical oxygen demand (COD), mg O_2/L	AWWA-4500OC	1,628.8
Biochemical oxygen demand (BOD_5), mg O_2/L	AWWA-5210B	786.5
BOD_5/COD	–	0.48
COD/TOC	–	0.92

2.3. Adsorption tests in a real textile industrial wastewater

biochar amount (100 mg), process temperature (25°C), and pH (3.0) were fixed according to previous results (presented in the supporting information) where a detailed optimization parameter design is performed to find the best operation conditions for biosorption of dyes on POP1 and POP2 materials. It was used 50.0 mL of composite sample of raw real wastewater in 100 mL Erlenmeyer flasks, using an isothermal water bath shaker (Autoshaking LABWIT ZWY-100H) under constant speed of 120 rpm. The pH of the initial solution was adjusted by adding NaOH or HCl solutions. After 24 h, the mixtures were separated by filtration. Additional adsorption tests were performed at pH 9.0. This pH value corresponds to the inherent condition of the real wastewater effluent. The remaining concentration of dyes was measured using a GENESYS 10S UV-Vis spectrophotometer at λ = 528, 431 and 620 nm for Reactive red 250, Reactive yellow 145 and Reactive blue 21, respectively. All experiments were performed by triplicate and for each variable an average value was obtained based on the three experiments carried out. The standard deviation (S) and Pearson's coefficient of relative variation (CV) were used as measures of absolute and relative dispersion between the three experiments, respectively. Table 3 shows nomenclature for the treatment conditions.

Spectroscopic characterization of raw textile wastewater was carried out from the transmittance data, the tristimulus values were evaluated and used to calculate the trichromatic coefficients, which were plotted on a chromaticity diagram in order to define the dominant wavelength and the hue purity conform to the procedure reported in APHA [43]. Decolorization performance was evaluated as % color removal efficiency from the absorbance readings at the three representative wavelengths and at the dominant wavelength. The removal of color in the real textile wastewater by the adsorption process was calculated by using Eq. (1).

$$\text{Colour removal}(\%) = \frac{\sum \text{Abs}_i - \sum \text{Abs}_f}{\sum \text{Abs}_i} \times 100 \quad (1)$$

where Abs_i and Abs_f are the initial absorbance and the absorbance at 24 h, respectively.

Physicochemical parameter removals were calculated according to Eq. (2).

Table 3
Type of wastewater and treatment reactions conditions

Wastewater code	Adsorption conditions
TIWW1	Textile industrial wastewater untreated.
TIWW2	Textile industrial wastewater treated at pH of 3.0 and biochar POP2.
TIWW3	Textile industrial wastewater treated at pH of 3.0 and biochar POP1.
TIWW4	Textile industrial wastewater treated at pH of 9.0 and biochar POP2.
TIWW5	Textile industrial wastewater treated at pH of 3.0 and activated carbon (CAC).

$$\text{Physicochemical parameter removal}(\%) = \frac{C_0 - C_f}{C_0} \times 100 \quad (2)$$

where C_0 and C_f are the initial and final concentration, respectively at adsorption time t.

Values obtained for the different physicochemical parameters for the real raw wastewater were compared with the values obtained for the samples once the treatment was completed. A comparison of achieve results was perform with the maximum acceptable values reported in the Colombian Environmental Regulations and in the Environmental Protection Agency (EPA) for an effluent from the textile industry [44,45].

3. Results and discussion

3.1. Physicochemical characterization of raw real textile wastewater

Fig. 1 reveals the spectrum in absorbance and transmittance mode of real raw wastewater. Four wavelengths of the different intervals of color distribution were identified (417, 523, 558 and 614 nm). Moreover, the dominant wavelength and purity defined from chromaticity diagram (Fig. 2a and b) are 535 nm and approximately 5%, respectively. In the other hand, the dominant l is in the interval of wavelengths of the red-purple hue (i.e., 530c–700 nm).

As regard as the low purity value, it is worth noting that a value of 100% purity corresponds to a condition where a color is represented by a single and unique wavelength, so far away from the wastewater under investigation, where the color content is distributed in a spectrum covering the interval 350–700 nm [46].

Average values for the physicochemical parameters evaluated are given in Table 4. The values reached for the standard deviation and the coefficient of variation in most of the physicochemical parameters evaluated in the two samplings for both the standard sample and the test sample were S ≤ 4.5 and CV ≤ 3.2%, respectively. These low values reflect that there were no very significant changes between the two samplings carried out.

The values obtained for BOD_5 and COD for the untreated wastewater are in the order of those reported for this type of effluent (80–9,273 mg O_2/L and 267–4,150 mg O_2/L for

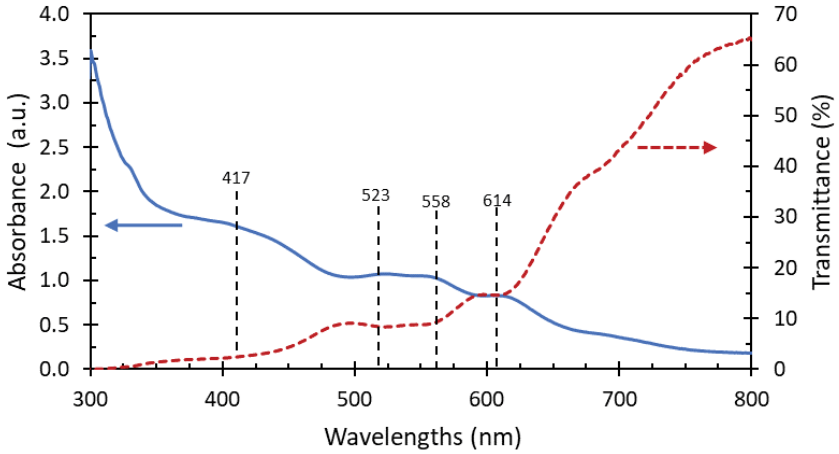

Fig. 1. Spectrum in absorbance and transmittance mode of real raw wastewater.

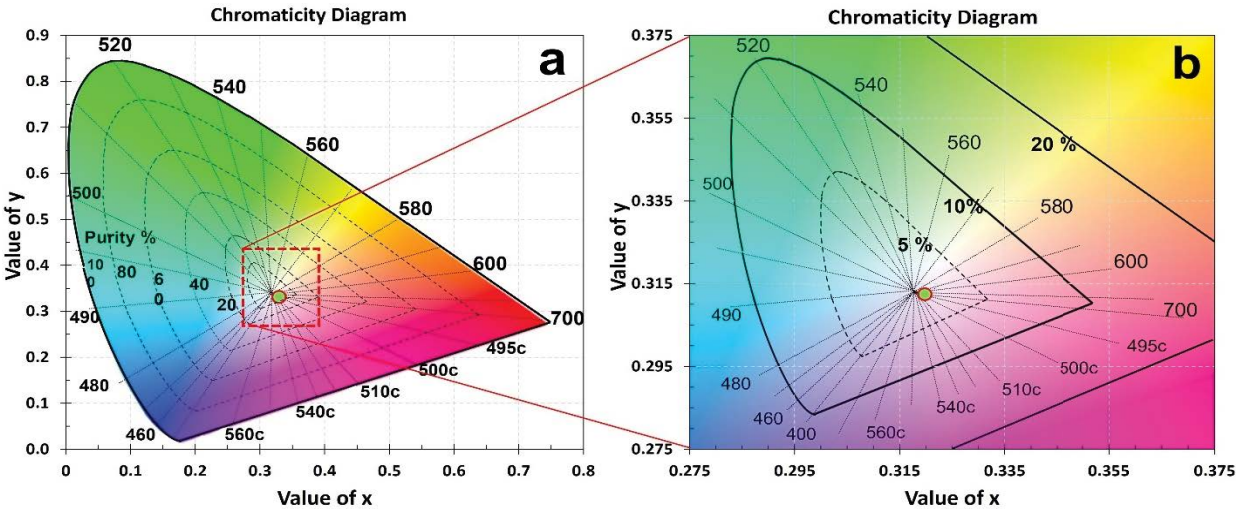

Fig. 2. Chromaticity diagram of real raw textile industrial wastewater.

Table 4
Physicochemical parameters evaluated under different conditions

Parameter/Unit	TIWW2	TIWW3	TIWW4	TIWW5	ER 00631	EPA 410.40
Color	Light-Black	Light-Black	Blue-Black	Blue-Black	–	–
True color (Pt-Co)	550	550	550	550	–	–
Temperature (°C)	25	25	25	25	–	–
pH (U of pH)	2.71	2.27	2.90	2.46	6.0–9.0	6.0–9.0
Turbidity (NTU)	80	69	53	97	–	–
Electrical conductivity (μS/cm)	29.1	39.3	38.1	36.7	–	–
Total solids (mg/L)	4,800	5,240	5,480	4,180	–	–
Total settleable solids (mg/L)	0	0	0	0	2.00	–
Total alkalinity (mg $CaCO_3$/L)	N.D	N.D	N.D	N.D	–	–
Total acidity (mg $CaCO_3$/L)	387.7	697.5	113.0	545.8	–	–
Total nitrates (mg NO_3^-/L)	185.2	176.7	154.5	136.3	–	–
Total chlorides (mg Cl^-/L)	1,100	1,150	1,000	1,200	1,200	–
Total copper (mg/L Cu)	0.16	0.12	0.19	0.17	1.00	–
Total chromium (mg/L Cr)	1.88	2.04	2.13	2.31	0.50	0.10
Total cadmium (mg/L Cd)	0.009	0.007	0.003	0.01	0.02	–
Total nickel (mg/L Ni)	0.03	0.02	0.02	0.03	0.50	–
Total zinc (mg/L Zn)	1.88	0.43	0.92	0.69	3.00	–
Total cobalt (mg/L Co)	0.200	0.182	0.198	0.235	0.50	–
TOC (mg O_2/L)	606.3	500.9	413.9	620.1	–	60.0
COD (mg O_2/L)	1,381.4	1,342.4	1,137.4	1,391.2	400.0	–
BOD_5 (mg O_2/L)	613.5	421.5	252.9	678.5	200.0	6.6
BOD_5/COD	0.44	0.31	0.22	0.49	–	–
COD/TOC	1.01	0.84	0.61	1.09	–	–

ER 00631: Permissible limits established by Colombian Resolution 0631 of the Ministry of Environment and Sustainable Development;
EPA: textile mills source category effluent limitations guidelines established by the Environmental Protection Agency;
N.D: No detectable.

BOD_5 and COD, respectively) [1,19,47,48]. In the case of TOC, its value exceeds all those found in the consulted literature (52–309 mg O_2/L) [12,19,48,49]. The calculated biodegradability index (taken as the BOD_5/COD ratio) was 0.48, indicating the presence of mostly inorganic matter, which can probably be attributed to the presence of an excess concentration of soluble salts and it also suggests that a significant part of the organic matter will be hardly biodegraded [46,48,50–52]. The low initial COD/TOC value of 0.92, indicates that the refractory organic compound content is very high. There are several studies in the literature that report low initial COD/TOC ratios for industrial wastewater, for instance Hansson et al. [53] reported an initial COD/TOC ratio below 2.

Additionally, the effluent shows a true color of 550 Pt-Co, which is within the range published in the literature (240–10,000 Pt-Co) [7,12,26,54–56]. The pH is ~ 10.0, a value close to those consulted in the bibliography for this type of wastewater, which are highly basic (8.5–12.4) [7,47,51,54,56]. Values reported in the literature for the turbidity of this type of wastewater are quite varied since values from 17.2 to 9251 NTU have been reported [7,51,54,56], the value found for raw wastewater in this study corresponds to 169 NTU. The electrical conductivity found (69.1 mS/cm) is very similar to most of the values reported in the literature (6.8–103 mS/cm) [51,54,48]. The value obtained for total solids is below those reported in the literature (5,420–116,468 mg/L) [48,51,54]. Additionally, it was not possible to measure total settleable solids. Alkalinity and acidity reflected values of 1,134 and 590.6 mg/L, respectively, however, there were no reported values for these parameters in the consulted bibliography. It is worth noting the high contents of

Table 5
Removal percentages and relationships of some parameters under different conditions

Parameter	Removal percentage of each parameter				
	TIWW1	TIWW2	TIWW3	TIWW4	TIWW5
Color	–	32.7	21.0	32.1	22.0
COD	–	15.2	17.6	30.2	14.6
BOD_5	–	20.2	46.4	67.8	13.7
TOC	–	29.1	41.4	51.6	27.4
Cu	–	36.0	52.0	24.0	32.0
Cr	–	26.8	20.6	17.1	10.1
Cd	–	85.0	85.0	85.0	65.0
Ni	–	25.0	50.0	50.0	25.0
Zn	–	51.0	88.8	76.0	82.0
Co	–	20.0	27.2	20.8	6.0

total nitrates (222.3 mg/L) and total chlorides (1,800 mg/L) are typical of most of those reported in the textile industry effluents (10.3–464 mg/L for nitrates and 745–1,912 mg/L for total chlorides) [8,46,47,54].

In addition, several heavy metals were identified at trace levels such as Cu (0.25 mg/L), Cr (2.57 mg/L), Cd (0.02 mg/L), Ni (0.04 mg/L), Zn (3.84 mg/L) and Co (0.250 mg/L). As for the Cu and Cr values, these are in the range reported in the literature (0.15–3.65 mg/L and 0.028–9.67 mg/L for Cu and Cr, respectively), while the values for Cd and Ni are above (0.088–0.88 mg/L and 0.124–7.57 mg/L for Cd and Ni, respectively) [57]. There were no reported values for the Co and Zn. In summary, the values obtained for all the physicochemical parameters evaluated in the real wastewater of the textile industry are among the ranges reported in the literature for this type of wastewater, which clearly shows that this study was carried out using a characteristic effluent of this sector.

The values obtained for parameters such as pH, Cl^-, Cr, Zn, COD and BOD_5 exceed the maximum permissible limit established in Colombian Regulations [44]. According to the data obtained from raw wastewater, it is established that the parameters like total settleable solids, Cu, Cd, Ni and Co comply with those established in Colombian Environmental Legislation [44]. Although, the Environmental Protection Agency establishes only maximum permissible limits for the pH, Cr, TOC and BOD_5 for this type of effluent, the raw real textile wastewater of this research comply no with theses parameters [45].

3.2. Adsorption tests in a real raw industrial wastewater

Fig. 3 reveals the color spectra recorded for the treatments with the different bioadsorbents, they give an idea of the evolution of the decolorization process with each investigated material. Furthermore, the highest color removal percentages were reached with the adsorbent POP2 under different pH value. In the case of POP1, the color removal percentages was similar than those obtained with CAC.

Similarly, no significant influence of the pH of the wastewater was identified on the removal percentages of this parameter using the different adsorbents. For instance, the achieved results with the biochar POP2 at pH 3 and 9 are almost the same (32.1% and 32.7%, respectively), additionally, both values are higher than those obtained with CAC (22.0%). On the other hand, the color removal percentage reached with POP1 is very similar to that obtained with CAC (21%), both at the same pH.

Furthermore, the higher removal percentages for COD, BOD_5 and TOC were achieved with the adsorbent POP2 at pH of 9.0, followed by POP1 at pH of 3.0 and finally POP2 at pH of 3.0. In all cases the removal percentages were similar or higher than those obtained with CAC. The highest values removal percentage were reached under basic conditions (pH = 9, inherent value of residual water), which suggests that it is not necessary to adjust this parameter to the optimal value established in previous studies. Although acceptable COD, BOD_5 and COD removal percentages were reached with POP2, it is necessary to carry out other additional treatments in order to comply with the maximum permissible limit values established in ER00631. As can be seen in Table 4, the obtained BOD_5/COD ratio decreased with overall biochars except with the CAC, expressing a slight decline in biotoxicity and an increment in the biodegradability of the wastewater after being treated.

Table 6 gathers the adsorption conditions, which are presented in descending order in relation to the removal percentage for each parameter evaluated. The results obtained in this study clearly evidence that a type of adsorbent under particular adsorption conditions can be effective for the removal of one or more pollutants, while for others not, which probably depends on the physical and chemical nature of both the adsorbent and the pollutant and the type of interactions that can occur between them. In this way it is not possible to affirm in this study that there is an ideal adsorbent for the treatment of a real wastewater for the complete removal of the different pollutants under evaluated conditions. This demonstrates the importance of evaluating

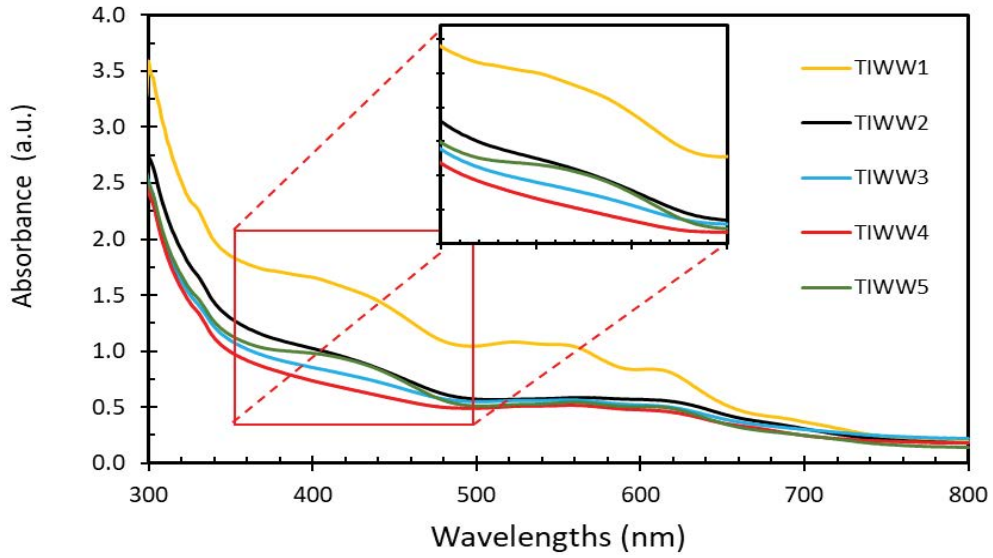

Fig. 3. UV-Vis absorbance spectra with different bioadsorbents.

Table 6
Adsorption conditions in descending order in relation to the removal percentage for each parameter evaluated

Parameter	Descending order
Color	TIWW2 ≈ TIWW4 < TIWW3 ≈ TIWW5
COD	TIWW4 > TIWW3 ≈ TIWW2 ≈ TIWW5
BOD_5	TIWW4 > TIWW3 > TIWW2 > TIWW5
TOC	TIWW4 > TIWW3 > TIWW2 > TIWW5
Cu	TIWW3 > TIWW2 ≈ TIWW5 ≈ TIWW4
Cr	TIWW2 > TIWW3 ≈ TIWW4 > TIWW5
Cd	TIWW4 > TIWW3 > TIWW4 ≈TIWW5
Ni	TIWW3 = TIWW4 > TIWW2 = TIWW5
Zn	TIWW3 > TIWW4 > TIWW5 > TIWW2
Co	TIWW3 > TIWW4 ≈ TIWW2 > TIWW5
Turbidity	TIWW4 > TIWW3 > TIWW2 = TIWW5
Electrical conductivity	TIWW2 > TIWW3 ≈ TIWW4 ≈ TIWW5
Nitrates	TIWW5 > TIWW4 > TIWW3 > TIWW2
Chlorides	TIWW4 > TIWW2 ≈ TIWW3 ≈ TIWW5

the effectiveness of an adsorbent under the real wastewater conditions with the presence of other pollutants, since it can present different phenomena of competition and inhibition between them by the different active sites that can affect the efficiency of the adsorbents.

In accordance with the pH value established in regulation ER00631, the wastewater treated with none of the adsorbents complies with the regulations. However, it is important to clarify those wastewaters were adjusted to a pH close to 3, since, in a previous study using response surfaces, the optimal conditions were found for which there is the greatest removal of different types of pollutants from the textile industry. In accordance with the data obtained for the settleable solids parameter according to the regulations for all wastewater samples, it is established that they all comply with the regulations, which indicates that, for this specific parameter, the use of extra treatments is not necessary. Based on the data of total nitrates, total acidity and total alkalinity, the regulations require the analysis and reporting of these parameters, for which data were obtained in a range of 130 and 230 mg NO_3^-/L, 110 mg $CaCO_3$/L and 700 mg $CaCO_3$/L, 1,113 and ND mg $CaCO_3$/L, respectively.

For the Cl^- parameter, the final treated wastewater with all adsorbent present values above the maximum permissible limit, which suggests that the use of other types of techniques is necessary to comply with the provisions of Colombian regulations. It is important to note that the total cadmium for raw wastewater (TIWW1) was in the maximum permissible limit, but in all tested cases was possible to establish values lower than 0.02 mg/L. The total cobalt for raw wastewater (TIWW1) was lower than the maximum permissible limit, however, but in all tested cases it was possible to decrease this parameter much more.

Total chromium for all wastewater samples do not comply with the provisions of the regulations. Although acceptable removal percentages were established, it is necessary to continue working on additional treatments that allow compliance with this parameter. For the total zinc parameter specifically for the TIWW1 sample, it does not comply with the maximum value established in the regulations. However, the wastewater TIWW2, TIWW3, TIWW4 and TIWW5 comply with this parameter, obtaining significant removal percentages and managing to establish this parameter under the maximum limits established by the standard.

Regarding the Cr removal percentage, it is observed that the removal of this component is favored under acidic conditions, additionally, greater removal of this contaminant was obtained with the synthesized materials compared to commercial activated carbon, even under basic conditions (without modification of the pH of the solution For the Ni parameter, it is The information was corrected. The information was corrected. observed that in addition to a relationship between the pH conditions and the removal results, the physicochemical properties of the material also influence, since using the same material at different pH values, greater removal is observed at basic conditions (pH = 9), however, very similar removals (50%) were obtained compared to another material under acidic conditions (pH = 3), which indicates a strong dependence on the physicochemical properties of the evaluated material, in addition to the pH conditions of wastewater.

In the case of Ni, the physicochemical properties of the material also influence, since using the same material at different pH values, greater removal percentage is observed at basic conditions (pH = 9) than at pH of 3.0, however, very similar removals (50%) were obtained in comparison with other material under acidic conditions (pH = 3), which indicates a strong dependence on the physicochemical properties of the evaluated material, in addition to the pH conditions of the wastewater. For Zn, a similar trend is observed in the dependence of pH with the % removal, since with the same material greater removal was observed at basic pH, however, it is not the predominant factor since with the other two materials obtained higher removal percentages. In general, it is observed that the synthesized materials, in most cases, are superior or similar to commercial activated carbon, for the removal of all the other parameters evaluated in this study, and the results obtained suggest that these materials are promising in the treatment and removal of some pollutants present in this type of industrial effluent such as industrial wastewater. In this way, it can be deduced that, although the results turn out to be promising, it is still necessary to look at alternatives that allow obtaining removal percentages of several parameters, in such a way that they can comply with the maximum permissible values in ER 00631 and can be discharged into surface waters or rivers.

The adsorption capacity and removal percentage of pollutants for the synthetized bioadsorbents in this study were compared with different adsorbents obtained from orange peel waste reported in the literature. According to the bibliography as is shown in Table 1, it is obvious that there is not any study on real raw wastewater from the textile industry using adsorbents derived from orange peel waste, moreover, there is little studies using simulated real industrial wastewater. In fact, in most studies carried out, ideal solutions with an only pollutant are used. Therefore, it is difficult to make a comparison. However, it is obvious that the performance of the synthesized adsorbents in this

investigation is good, since the maximum adsorption capacity in term of color removal were higher or very similar to those gathered in the Table 1 and conducted in a simulated wastewater. Although, as seen also in the same Table 1, the maximum adsorption capacity of the obtained adsorbents in this research is lower than other studies carried out using ideal solutions containing only the dye, which could be due to the presence of a large number of other compounds such as NaCl, Na_2CO_3 and NaOH that compete with the dye for the adsorption sites and therefore, this would lead to obtain less capacities of adsorption (See the supporting information). Thus, it should be noted that the adsorption capacity is highly dependent on the type of matrix analyzed, the physicochemical properties of the adsorbent and the operating conditions.

3.3. Biochars characterization

XRD patterns of the POP1 and POP2 shown in Fig. 4 evidently explicates the presence of amorphous materials due to hemicellulose and lignin of the orange peels. The presence of crystalline peaks at 23.4° and 44.5° indicates the crystalline nature of cellulosic material [26,35]. Nascimento et al. [58], obtained diffraction peaks indicating that the samples have a turbostratic structure.

Meanwhile, the BET analysis of the bioadsorbent indicated a surface area of 5.0, 8.0 and 650 m^2/g, for POP1, POP2 and CAC, respectively (Table 7), the area surface of orange peels biocarbones is slightly lesser than the value reported in the literature [30,39]. In addition, it can be noticed that there are similarities in the textural properties of the synthetized biomaterials (POP1 and POP2), where the differences even in the values of the specific surface area are within the experimental error of the technique (±20 m^2/g). However, it is highlighted that the surface area of CAC was ~ 81-fold higher in comparison with POP1 and POP2.

Table 8 displays the moisture and ash content, volatile matter, the fixed carbon and the biochar yield. The moisture content of both POP1 and POP2 adsorbents were found to be ~7.0% and 10% respectively, which is slightly higher than the value reported by Benaissa et al. [39,59] and Temesgen et al. [30]. The ash content for both bioadsorbent is relatively high compared to literature data (30.0% and 18.5% for POP1 and POP2, respectively), since the residual organic compounds present in the adsorbents from agricultural products is in the range 0.2% to 13.4%, [39,60] which indicates that the amount of inorganic substituent present is slightly high. The volatile matter was 17.9% and 10.3% for POP1 and POP2, respectively, this was lower (34%–44%) than reported for biomaterials of orange peel waste [29,30].

Regarding isoelectric point (Table 7), it was 4.5 and 4.8 for POP1 and POP2, respectively. At solution pH values below the pH_{PZC} value, it is promoting the adsorption of anions because the surface of solid materials is positively charged.

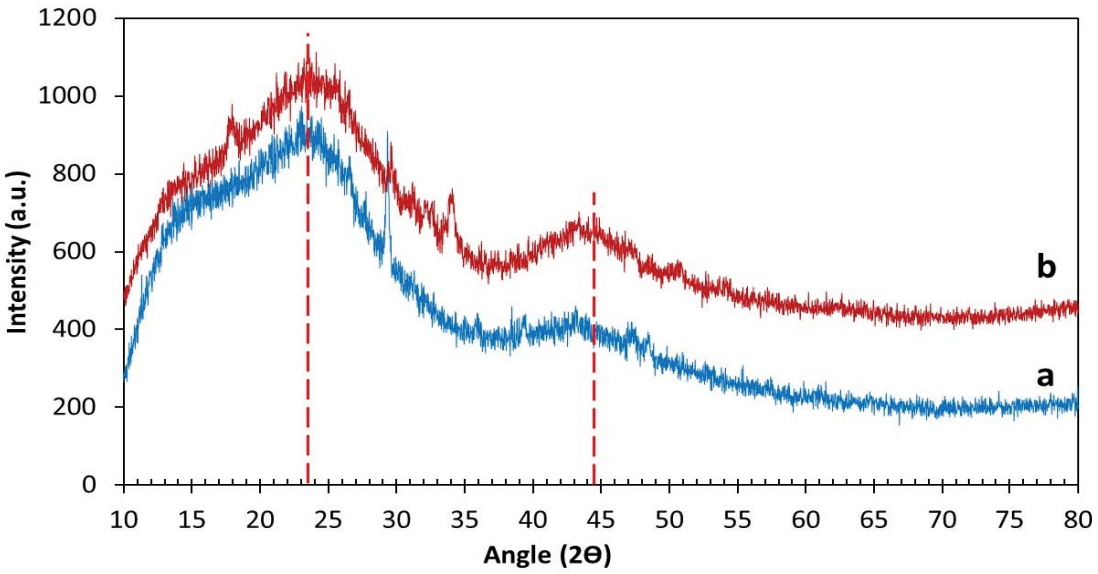

Fig. 4. XRD patterns of bioadsorbents: (a) POP1 and (b) POP2.

Table 7
Physicochemical properties and elemental analysis of the bioadsorbents

Adsorbent	Isoelectric point	Surface area (m^2/g)	Pore volume (cm^3/g)	Pore diameter (nm)	Elemental composition (wt.%)						
					N	C	H	S	O	H/C	O/C
POP1	4.5	5.0	0.002	1.86	0	42.9	0.73	1.76	54.6	0.02	1.27
POP2	4.8	8.0	0.004	1.77	0	19.8	2.30	1.84	76.1	0.12	3.84
CAC	–	650	0.940	41.1	1.1	73.7	1.6	–	–	0.02	–

The pH_{PZC} is probably another factor that influenced the obtaining of low removal percentages for the pollutants examined [30,33,40]. It is well known that the pyrolysis temperature strongly effects the biochar production yield. In this study, the char yield, slight increased with increasing temperature from 500°C to 700°C, it might be because the higher the temperature there is greater destruction of chemical constituents, such as cellulose and hemicelluloses, which is consistent with the elemental composition results and with the yields with other biochar obtained from orange peels, indicating that our findings are similar results those reported for other studies [61–64].

The elemental analysis showed that both biomaterials were dominated by carbon and oxygen and small amounts of hydrogen and sulphur-free. Nitrogen was not detected probably due to the presence of a very low nitrogen content that was below the detection limit of the CHNS analyzer. The high carbon content, low H/C and O/C ratio of both biomaterials indicate improved resistance toward oxidation and chemical reactions due to the presence of strong carbon bonding [24,29].

According to the literature [61] the ash content of the POP1 and POP2 materials is medium (5%–10%) and high (>10%). The H/C ratio is frequently used as an indicator of the degree of aromaticity and saturation of the biomass, which, in turn, is related to its great stability in the environment. The H/C ratios for our materials are 0.02 and 0.12 for POP1 and POP2, respectively, indicating a graphite-like structure in the obtained biofuels. Similar results have been reported in the literature [61]. On the other hand, the thermal profile of both bioadsorbents showed three stages of weight loss. The first stage around 100°C corresponds to the loss of occluded or adsorbed water molecules with a percentage of 7.10% and 10.32% for POP1 and POP2, respectively. The second stage (between 150°C and 800°C) with a maximum percentage weight loss of 17.9% and 10.3% for POP1 and POP2, respectively, is commonly related to the thermal decomposition of hemicellulose and glycosidic bonds β-(1→4) from the cellulose. The third stage above 800°C is associated with the decomposition of aromatic structures and the remaining cellulose and lignin.

The surface functional groups of the POP1, POP2 and CAC adsorbents were studied before and after adsorption by using FTIR spectroscopy, these spectra are depicted in Figs. 5 and 6. The spectra of all materials are very similar. The absorption strong and wide bands at 3,890 and 3,720 cm^{-1}, can be attributed to the stretching vibration of the hydroxyl groups bond (–OH) of a large number of functional groups (alcohol, phenolic and carboxylic groups) derived from cellulose, pectin, hemicellulose, lignin [63]. The band at 3,620 cm^{-1} is related with to the stretching vibration of CH bonds, which appear in the range 3,000–3,690 cm^{-1}) [62]. The band around 2860 cm^{-1} are related to the stretching vibration of CH bonds in methyl and methylene [63]. The band at 1,720 cm^{-1} is assigned to C=O ester group [62]. The band at approximately 1,690 cm^{-1} is due to functional group C=O (ketone, aldehydes, amides) [63]. The band observed at 1,517 cm^{-1} is assigned to C=O stretching vibration. The band at 1,160 cm^{-1}

Table 8
Proximal analysis result of the bioadsorbents and mass yield

Adsorbent	Parameter (wt.%)				
	Moisture content	Ash content	Volatile matter	Fixed carbon	Biochar yield
POP1	7.1	30.0	17.9	65.7	9.0
POP2	10.3	18.5	10.3	66.5	13.0

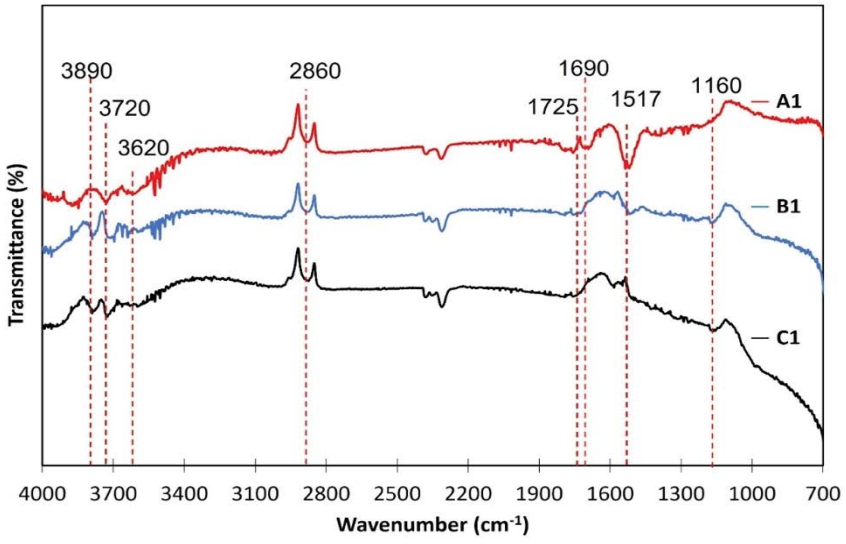

Fig. 5. FTIR spectrum of adsorbents before treatment adsorption. A1: POP1, B1: POP2, and C1: CAC.

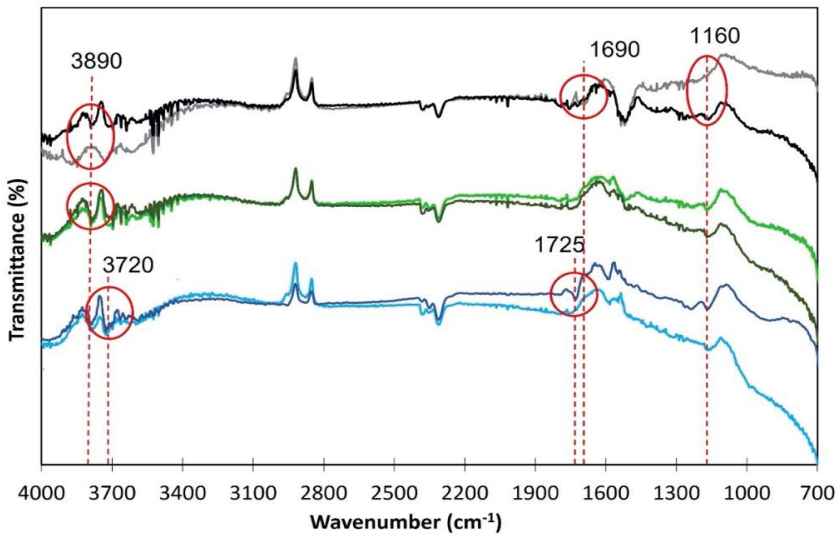

Fig. 6. FTIR spectrum comparisons of adsorbents before (A1, B1 and C1) and after treatment adsorption (A2, B2 and C2). A2: POP1, B2: POP2, and C2: CAC.

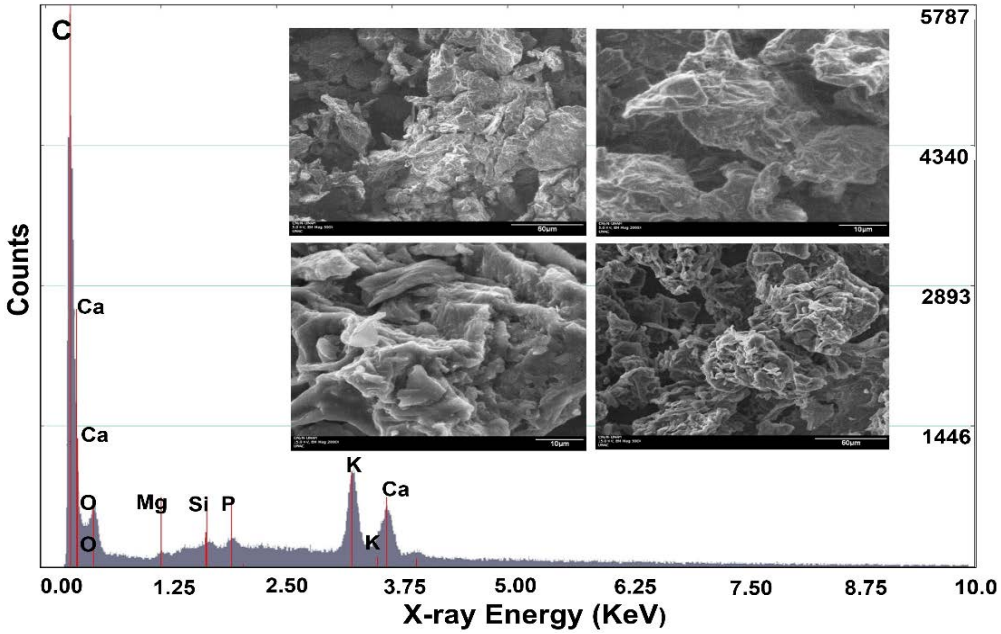

Fig. 7. SEM images and EDAX spectrum of POP1.

can be assigned to the vibrations of the C–O–C and OH groups of polysaccharides [63].

FTIR spectrum of POP1 and POP2 showed a similar pattern between them, except for the bands at 1,160 cm^{-1} and 3,890 cm^{-1} that appear only in the POP2 material and the band at 1,690 cm^{-1} that appears only in the POP1 adsorbent. Finally, in the material POP2 the band at 1,517 cm^{-1} decreased significantly compared to POP1. This may be caused by the thermally treatments applied are different. Moreover, comparing the spectra of POP1, POP1 and CAC. When comparing CAC with POP2, no significant differences are observed in the spectra, except that in the CAC material the band at 1,517 cm^{-1} (N–O nitro) is not clearly evident. Several differences were also identified between the spectra of POP1 and CAC, the bands at 3,890 and 1,160 cm^{-1} appear only in the CAC, while the bands located at 1,690 and 1,517 cm^{-1} are observed only in the POP1 material.

By comparing POP1 before and after adsorption, the bands appear at 3,890 and 1,160 cm^{-1} and the band disappears at 1,690 cm^{-1}, after adsorption. When comparing POP2 before and after adsorption, no significant differences are observed, except that the intensity of the band located at 3,890 cm^{-1} increases slightly after adsorption. Finally, when comparing the CAC before and after adsorption, an increase

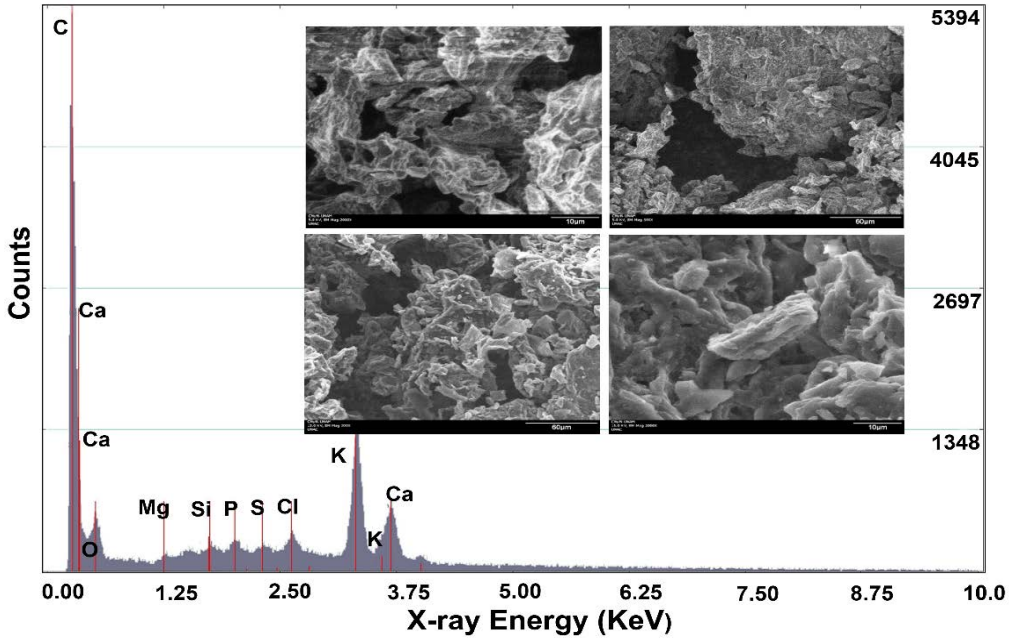

Fig. 8. SEM images and EDAX spectrum of POP2.

in the intensity of the band located at 3,720 cm^{-1} is observed after adsorption, additionally the intensity of the band 2,860 cm^{-1} decreases, and a band appears at 1,780 cm^{-1}.

The results of SEM/energy-dispersive X-ray analysis of the biochars are shown in Figs. 7 and 8. It can observe the surface morphology of two bioadsorbents was similar to each other as well as their elemental composition. A layered structure on the surface of adsorbent and rough morphology was displayed, also the biochars are not very porous, which confirms the results obtained in the BET analyzes [23,26].

In summary, the physicochemical characterization results of the bioadsorbents obtained at different temperatures, no showed significant differences in terms of chemical composition, morphology, structure, and textural properties, which could explain the reason for the small differences between the coloration removal percentages and in the other physicochemical parameters with the two evaluated materials. Therefore, the results obtained clearly show that in the processes of adsorption and removal of pollutants present in a real industrial wastewater, the surface area and composition biomaterial are not the only determining parameter, but also the nature of the pollutants, since despite the fact that commercial activated carbon had a significantly higher surface area than the synthesized bioadsorbents in this investigation, the material used like reference had a lower performance in terms of removal percentages for the most of analyzed pollutants.

4. Conclusions

The values obtained for all the physicochemical parameters evaluated in the real wastewater of the textile industry are among the ranges reported in the literature for this type of wastewater, which clearly shows that this study was carried out using a characteristic effluent of this sector.

The treatments applied with the different adsorbents evaluated allowed to significantly decrease the removal of parameters such as Cl^- and Zn, complying with the provisions of the same environmental regulations, however, it is necessary to evaluate other conditions or additional treatments to achieve removals in terms of pH, Cr, COD and BOD_5 that allow obtaining values lower than the maximum permissible limits regulated by Colombian regulations.

These results reveal small differences in the performances of the two obtained adsorbents from orange peel waste. These must be since the surface texture, porosity, surface chemistry and composition of the chars are very similar. However, it is evident that all the biochars showed a better performance in the pollutant removal compared to the commercial activated carbon. Thus, this work shows that the orange waste transformed adsorbent could compete with available commercial adsorbents for the treatment of industrial textile wastewater, however, is necessary to know the adsorption capacity, desorption capability and reusability of the bioadsorbents.

Acknowledgments

We are grateful for the financial support from the Politécnico Colombiano Jaime Isaza Cadavid, Colombia.

Declaration of competing interest

The authors declare that they have no known competing financial interests or personal relationships that could have appeared to influence the work reported in this paper.

References

[1] L. Hossain, S.K. Sarker, M.S. Khan, Evaluation of present and future wastewater impacts of textile dyeing industries in Bangladesh, Environ. Dev., 26 (2018) 23–33.

[2] B. Liu, J. Wu, C. Cheng, J. Tang, M.F.S. Khan, J. Shen, Identification of textile wastewater in water bodies by fluorescence excitation emission matrix-parallel factor analysis and high-performance size exclusion chromatography, Chemosphere, 216 (2019) 617–623.
[3] P.H. Nakhate, C.R. Gadipelly, N.T. Joshi, K.V. Marathe, Engineering aspects of catalytic ozonation for purification of real textile industry wastewater at the pilot scale, J. Ind. Eng. Chem., 69 (2019) 77–89.
[4] K. Nadeem, G.T. Guyer, B. Keskinler, N. Dizge, Investigation of segregated wastewater streams reusability with membrane process for textile industry, J. Cleaner Prod., 228 (2019) 1437–1445.
[5] R. Shoukat, S.J. Khan, Y. Jamal, Hybrid anaerobic-aerobic biological treatment for real textile wastewater, J. Water Process Eng., 29 (2019) 1–8.
[6] I. Khouni, G. Louhichi, A. Ghrabi, Assessing the performances of an aerobic membrane bioreactor for textile wastewater treatment: influence of dye mass loading rate and biomass concentration, Process Saf. Environ. Prot., 135 (2020) 364–382.
[7] U. Sathya, Keerthi, M. Nithya, N. Balasubramanian, Evaluation of advanced oxidation processes (AOPs) integrated membrane bioreactor (MBR) for the real textile wastewater treatment, J. Environ. Manage., 246 (2019) 768–775.
[8] E.B. Arikan, Z. Isik, H.D. Bouras, N. Dizge, Investigation of immobilized filamentous fungi for treatment of real textile industry wastewater using up flow packed bed bioreactor, Bioresour. Technol. Rep., 7 (2019) 1–6.
[9] N. Bougdour, R. Tiskatine, I. Bakas, A. Assabbane, Photocatalytic degradation of industrial textile wastewater using $S_2O_8^{2-}/Fe^{2+}$ process, Mater. Today:. Proc., 22 (2020) 69–72.
[10] J. Núñez, M. Yeber, N. Cisternas, R. Thibaut, P. Medina, C. Carrasco, Application of electrocoagulation for the efficient pollutants removal to reuse the treated wastewater in the dyeing process of the textile industry, J. Hazard. Mater., 371 (2019) 705–711.
[11] M. Rajasimman, S.V. Babu, N. Rajamohan, Biodegradation of textile dyeing industry wastewater using modified anaerobic sequential batch reactor – start-up, parameter optimization and performance analysis, J. Taiwan Inst. Chem. Eng., 72 (2017) 171–181.
[12] P. Kaur, J.P. Kushwaha, V.K. Sangal, Electrocatalytic oxidative treatment of real textile wastewater in continuous reactor: degradation pathway and disposability study, J. Hazard. Mater., 346 (2018) 242–252.
[13] M. Mousazadeh, S.M. Alizadeh, Z. Frontistis, I. Kabdaşlı, E. Karamati Niaragh, Z. Al Qodah, Z. Naghdali, A.E.D. Mahmoud, M.A. Sandoval, E. Butler, M.M. Emamjomeh, Electrocoagulation as a promising defluoridation technology from water: a review of state of the art of removal mechanisms and performance trends, Water (Switzerland), 13 (2021) 656, doi: 10.3390/w13050656.
[14] H. Hayat, Q. Mahmood, A. Pervez, Z.A. Bhatti, S.A. Baig, Comparative decolorization of dyes in textile wastewater using biological and chemical treatment, Sep. Purif. Technol., 154 (2015) 149–153.
[15] R. Kiani, F. Mirzaei, F. Ghanbari, R. Feizi, F. Mehdipour, Real textile wastewater treatment by a sulfate radicals-advanced oxidation process: peroxydisulfate decomposition using copper oxide (CuO) supported onto activated carbon, J. Water Process Eng., 38 (2020) 101623, doi: 10.1016/j.jwpe.2020.101623.
[16] P.R. Souza, G.L. Dotto, N.P.G. Salau, Artificial neural network (ANN) and adaptive neuro-fuzzy interference system (ANFIS) modelling for nickel adsorption onto agro-wastes and commercial activated carbon, J. Environ. Chem. Eng., 6 (2018) 7152–7160.
[17] P. Srinivasan, A. John Bosco, R. Kalaivizhi, J. Arockia Selvi, P. Sivakumar, Adsorption isotherm and kinetic study of Direct Orange 102 dyes on TNJ activated carbon, Mater. Today:. Proc., 34 (2021) 389–394.
[18] A.M. Herrera-González, M. Caldera-Villalobos, A.A. Peláez-Cid, Adsorption of textile dyes using an activated carbon and crosslinked polyvinyl phosphonic acid composite, J. Environ. Manage., 234 (2019) 237–244.
[19] S. Bener, S. Atalay, G. Ersöz, The hybrid process with eco-friendly materials for the treatment of the real textile industry wastewater, Ecol. Eng., 148 (2020) 1–12.
[20] M. Wakkel, B. Khiari, F. Zagrouba, Textile wastewater treatment by agro-industrial waste: equilibrium modelling, thermodynamics and mass transfer mechanisms of cationic dyes adsorption onto low-cost lignocellulosic adsorbent, J. Taiwan Inst. Chem. Eng., 96 (2019) 439–452.
[21] R.B. Gapusan, M.D.L. Balela, Adsorption of anionic methyl orange dye and lead(II) heavy metal ion by polyaniline-kapok fiber nanocomposite, Mater. Chem. Phys., 243 (2020), doi: 10.1016/j.matchemphys.2020.122682.
[22] N. Mahato, K. Sharma, M. Sinha, E.R. Baral, R. Koteswararao, A. Dhyani, M. Hwan Cho, S. Cho, Bio-sorbents, industrially important chemicals and novel materials from citrus processing waste as a sustainable and renewable bioresource: a review, J. Adv. Res., 23 (2020) 61–82.
[23] V.S.S. Munagapati, J.-C. Wen, C.-L. Pan, Y. Gutha, J.-H. Wen, Enhanced adsorption performance of Reactive red 120 azo dye from aqueous solution using quaternary amine modified orange peel powder, J. Mol. Liq., 285 (2019) 375–385.
[24] P.N.Y. Yek, W. Peng, C.C. Wong, R.K. Liew, Y.L. Ho, W.A. Wan Mahari, E. Azwar, T.Q. Yuan, M. Tabatabaei, M. Aghbashlo, C. Sonne, S.S. Lam, Engineered biochar via microwave CO_2 and steam pyrolysis to treat carcinogenic Congo red dye, J. Hazard. Mater., 395 (2020) 122636, doi: 10.1016/j.jhazmat.2020.122636.
[25] N. Tavker, M. Sharma, Designing of waste fruit peels extracted cellulose supported molybdenum sulfide nanostructures for photocatalytic degradation of RhB dye and industrial effluent, J. Environ. Manage., 255 (2020) 1–12.
[26] M. Ahmed, F. Mashkoor, A. Nasar, Development, characterization, and utilization of magnetized orange peel waste as a novel adsorbent for the confiscation of crystal violet dye from aqueous solution, Groundwater Sustainable Dev., 10 (2020) 100–322.
[27] X. Chen, H. Li, W. Liu, X. Zhang, Z. Wu, S. Bi, W. Zhang, H. Zhan, Effective removal of methyl orange and rhodamine B from aqueous solution using furfural industrial processing waste: furfural residue as an eco-friendly biosorbent, Colloids Surf., A, 583 (2019) 123976, doi: 10.1016/j.colsurfa.2019.123976.
[28] M.A. Ahmad, N.B. Ahmed, K.A. Adegoke, O.S. Bello, Sorption studies of methyl red dye removal using lemon grass (*Cymbopogon citratus*), Chem. Data Collect., 22 (2019) 1–11.
[29] S.S. Lam, R.K. Liew, Y.M. Wong, P.N.Y. Yek, N.L. Ma, C.L. Lee, H.A. Chase, Microwave-assisted pyrolysis with chemical activation, an innovative method to convert orange peel into activated carbon with improved properties as dye adsorbent, J. Cleaner Prod., 162 (2017) 1376–1387.
[30] F. Temesgen, N. Gabbiye, O. Sahu, Biosorption of Reactive red dye (RRD) on activated surface of banana and orange peels: economical alternative for textile effluent, Surf. Interfaces, 12 (2018) 151–159.
[31] M.H. Munawer, H.L. Chee, P.L. Kiew, Magnetized orange peel: a realistic approach for methylene blue removal, Mater. Today:. Proc., 47 (2021), doi: 10.1016/j.matpr.2021.02.796.
[32] P.S. Kumar, P.S.A. Fernando, R.T. Ahmed, R. Srinath, M. Priyadharshini, A.M. Vignesh, A. Thanjiappan, Effect of temperature on the adsorption of methylene blue dye onto sulfuric acid–treated orange peel, Chem. Eng. Commun., 201 (2014) 1526–1547.
[33] G.E. do Nascimento, M.M.M.B. Duarte, N.F. Campos, O.R.S. da Rocha, V.L. da Silva, Adsorption of azo dyes using peanut hull and orange peel: a comparative study, Environ. Technol., 35 (2014) 1436–1453.
[34] S. Hashemian, K. Salari, H. Salehifar, Z. Yazdi, Removal of azo dyes (Violet B and Violet 5R) from aqueous solution using new activated carbon developed from orange peel, J. Chem., 2013 (2013) 1–10.
[35] A. Guediri, A. Bouguettoucha, D. Chebli, N. Chafai, A. Amrane, Molecular dynamic simulation and DFT computational studies on the adsorption performances of methylene blue in aqueous solutions by orange peel-modified phosphoric acid,

J. Mol. Struct., 1202 (2020) 127290, doi: 10.1016/j.molstruc.2019.127290.
[36] V.S. Munagapati, D.-S. Kim, Adsorption of anionic azo dye Congo red from aqueous solution by cationic modified orange peel powder, J. Mol. Liq., 220 (2016) 540–548.
[37] K. Yoon, D.-W. Cho, A. Bhatnagar, H. Song, Adsorption of As(V) and Ni(II) by Fe-Biochar composite fabricated by co-pyrolysis of orange peel and red mud, Environ. Res., 188 (2020) 109809, doi: 10.1016/j.envres.2020.109809.
[38] S. Pavithra, G. Thandapani, Sugashini S, Sudha P.N., H.H. Alkhamis, A.F. Alrefaei, M.H. Almutairi, Batch adsorption studies on surface tailored chitosan/orange peel hydrogel composite for the removal of Cr(VI) and Cu(II) ions from synthetic wastewater, Chemosphere, 271 (2021) 129415, doi: 10.1016/j.chemosphere.2020.129415.
[39] E. Safari, N. Rahemi, D. Kahforoushan, S. Allahyari, Copper adsorptive removal from aqueous solution by orange peel residue carbon nanoparticles synthesized by combustion method using response surface methodology, J. Environ. Chem. Eng., 7 (2019) 102847, doi: 10.1016/j.jece.2018.102847.
[40] S. Guiza, Biosorption of heavy metal from aqueous solution using cellulosic waste orange peel, Ecol. Eng., 99 (2017) 134–140.
[41] Y. Chen, H. Wang, W. Zhao, S. Huang, Four different kinds of peels as adsorbents for the removal of Cd(II) from aqueous solution: kinetics, isotherm and mechanism, J. Taiwan Inst. Chem. Eng., 88 (2018) 146–151.
[42] R. Acosta, D. Nabarlatz, A. Sánchez-Sánchez, J. Jagiello, P. Gadonneix, A. Celzard, V. Fierro, Adsorption of Bisphenol A on KOH-activated tyre pyrolysis char, J. Environ. Chem. Eng., 6 (2018) 823–833.
[43] R.B. Baird, A.D. Eaton, E.W. Rice, Standard Methods for the Examination of Water and Wastewater, 2015. Available at: https://doi.org/10.1016/B978-0-12-382165-2.00237-3
[44] M. de A. y D. Sostenible, Resolución 0631 del 17 de marzo de 2015, "Por La Cual Se Establ. Los Parámetros y Los Valores Lpimite Máximos Permis. En Los Vertimientos Puntuales a Cuerpos Agua Supeficiales y a Los Sist. Alcantarilladopúblico y Se Dictan Otras Disposiciones.", 2015, pp. 1–62.
[45] Environmental Protection Agency, Part 410 — Textile Mills Point Source Category, Environ. Prot. Agency, 31 (2020) 175–177.
[46] M.C. Tomei, J. Soria Pascual, D. Mosca Angelucci, Analysing performance of real textile wastewater bio-decolorization under different reaction environments, J. Cleaner Prod., 129 (2016) 468–477.
[47] M.C. Tomei, D. Mosca Angelucci, A.J. Daugulis, Sequential anaerobic-aerobic decolorization of a real textile wastewater in a two-phase partitioning bioreactor, Sci. Total Environ., 573 (2016) 585–593.
[48] N. Nippatla, L. Philip, Electrocoagulation–floatation assisted pulsed power plasma technology for the complete mineralization of potentially toxic dyes and real textile wastewater, Process Saf. Environ. Prot., 125 (2019) 143–156.
[49] N. Jaafarzadeh, A. Takdastan, S. Jorfi, F. Ghanbari, M. Ahmadi, G. Barzegar, The performance study on ultrasonic/Fe_3O_4/H_2O_2 for degradation of azo dye and real textile wastewater treatment, J. Mol. Liq., 256 (2018) 462–470.
[50] O.O. Oyebamiji, W.J. Boeing, F.O. Holguin, O. Ilori, O. Amund, Green microalgae cultured in textile wastewater for biomass generation and biodetoxification of heavy metals and chromogenic substances, Bioresour. Technol. Rep., 7 (2019) 100247, doi: 10.1016/j.biteb.2019.100247.
[51] S. Jorfi, G. Barzegar, M. Ahmadi, R. Darvishi Cheshmeh Soltani, N. Alah Jafarzadeh Haghighifard, A. Takdastan, R. Saeedi, M. Abtahi, Enhanced coagulation-photocatalytic treatment of Acid red 73 dye and real textile wastewater using UVA/synthesized MgO nanoparticles, J. Environ. Manage., 177 (2016) 111–118.
[52] F.Y. Aljaberi, The most practical treatment methods for wastewaters: a systematic review, Mesopotemia Environ. J., 5 (2018) 1–28.
[53] H. Hansson, F. Kaczala, M. Marques, W. Hogland, Photo-Fenton and Fenton oxidation of recalcitrant industrial wastewater using nanoscale zero-valent iron, Int. J. Photoenergy, 2012 (2012) 531076, doi: 10.1155/2012/531076.
[54] I.M.S. Pillai, A.K. Gupta, Performance analysis of a continuous serpentine flow reactor for electrochemical oxidation of synthetic and real textile wastewater: energy consumption, mass transfer coefficient and economic analysis, J. Environ. Manage., 193 (2017) 524–531.
[55] E. Sanmuga Priya, P. Senthamil Selvan, Water hyacinth (*Eichhornia crassipes*) – an efficient and economic adsorbent for textile effluent treatment – a review, Arabian J. Chem., 10 (2017) S3548–S3558.
[56] N.R. Khandaker, I. Afreen, D.S. Diba, F.B. Huq, T. Akter, Treatment of textile wastewater using calcium hypochlorite oxidation followed by waste iron rust aided rapid filtration for color and COD removal for application in resources challenged Bangladesh, Groundwater Sustainable Dev., 10 (2020) 100342, doi: 10.1016/j.gsd.2020.100342.
[57] S. Bener, Ö. Bulca, B. Palas, G. Tekin, S. Atalay, G. Ersöz, Electrocoagulation process for the treatment of real textile wastewater: effect of operative conditions on the organic carbon removal and kinetic study, Process Saf. Environ. Prot., 129 (2019) 47–54.
[58] G.E. do Nascimento, M.M.M.B. Duarte, N.F. Campos, O.R.S. da Rocha, V.L. da Silva, Adsorption of azo dyes using peanut hull and orange peel: a comparative study, Environ. Technol., 35 (2014) 1436–1453.
[59] H. Benaïssa, Removal of acid dyes from aqueous solutions using orange peel as a sorbent material, Int. J. Environ. Pollut., 34 (2008) 71–82.
[60] F.F. Avelar, M.L. Bianchi, M. Gonçalves, E.G. da Mota, The use of piassava fibers (*Attalea funifera*) in the preparation of activated carbon, Bioresour. Technol., 101 (2010) 4639–4645.
[61] G. Stella Mary, P. Sugumaran, S. Niveditha, B. Ramalakshmi, P. Ravichandran, S. Seshadri, Production, characterization and evaluation of biochar from pod (*Pisum sativum*), leaf (*Brassica oleracea*) and peel (*Citrus sinensis*) wastes, Int. J. Recycl. Org. Waste Agric., 5 (2016) 43–53.
[62] B. Chen, Z. Chen, Sorption of naphthalene and 1-naphthol by biochars of orange peels with different pyrolytic temperatures, Chemosphere, 76 (2009) 127–133.
[63] A.G. Adeniyi, J.O. Ighalo, D.V. Onifade, Biochar from the thermochemical conversion of orange (*Citrus sinensis*) peel and albedo: product quality and potential applications, Chem. Afr., 3 (2020) 439–448.
[64] T.K. Oh, B.S. Choi, Y. Shinogi, J. Chikushi, Characterization of biochar derived from three types of biomass, J. Fac. Agric. Kyushu Univ., 57 (2012) 61–66.

Supplemental information

S1. Preliminary adsorption tests in a synthetic industrial wastewater

The adsorption efficiency of the biochars was evaluated for the treatment of a synthetic industrial wastewater. Thus, first the preliminary batch adsorption process using the POP1 and POP2 bioadsorbent were conducted to achieve the optimum operating conditions for the dye adsorption (Reactive red 250, Reactive yellow 145 and Reactive blue 21).

The elemental composition of the textile wastewater simulated in the laboratory was set with data provided by a textile industry factory (Table S1).

Different parameters, including biochar amount (25–100 mg), adsorption temperature (25°C–45°C), and pH (3–12), were studied using 50.00 mL of synthetic industrial wastewater in 100 mL Erlenmeyer flasks in an isothermal water bath shaker (Autoshaking LABWIT ZWY-100H) under constant speed of 120 rpm. The pH of the initial solution was adjusted by adding 0.1 mol/L NaOH or 0.1 mol/L HCl solutions. After 24 h, the mixtures were separated by filtration. The remaining dye concentration was measured using a GENESYS 10S UV-Vis spectrophotometer at λ = 528, 431 and 620 nm for Reactive red 250, Reactive yellow 145 and Reactive blue 21, respectively.

The color removal in the simulated textile wastewater by the adsorption process was calculated using Eq. (1).

$$\text{Colour removal}\left(\%\right) = \frac{\text{Abs}_0 - \text{Abs}_f}{\text{Abs}_0} \times 100 \tag{S1}$$

where Abs_0 and Abs_f are the initial absorbance and the absorbance at adsorption time t, respectively.

S2. Design of experiments

Different adsorption tests were carried out to determine the effect of three factors: pH solution, temperature, and amount of bioadsorbent. The factors and levels for experimentation are presented in Table S2. A Box–Behnken design with a 95% confidence level was implemented to find the optimal operating points in the removal of three dyes in simulated textile wastewater. This type of design was implemented because a spherical arrangement of the points is the most efficient when looking for the best conditions of a process once the factors affecting the process are known.

Table S1
Composition of simulated textile wastewater

Chemical	Concentration (g/L)
Dye	0.1
NaCl	50
Na_2CO_3	15
NaOH	1.5

Table S2
Factors and levels of experimental design

Factors	Unit	Symbol	Levels		
			Low (–1)	Medium (0)	High (+1)
pH	U of pH	*A*	3.0	7.0	12.0
Temperature	°C	*B*	25	35	45
Amount of adsorbent	mg	*C*	25	50	100

S3. Results and discussion

The Eq. (2) represents the empirical relationship between dye removal efficiency and input variables expressed by the quadratic model, where *A*, *B* and *C* are temperature, synthetic wastewater pH, and amount of adsorbent, respectively. The coefficient values in this equation indicate the intensity and the sign of coefficient present the positive or negative influence of the input variable on the dye removal percentage. A positive effect of a factor means that when the factor level increases, the dye removal percentage is improved and vice versa.

$$\begin{aligned}\text{Dye removal}\left(\%\right) = {} & 32.5415 - 0.0101444A + 3.57674B \\ & + 0.943273C + 0.00378889A^2 + 0.0192848AB \\ & - 0.0155568AC - 0.135105B^2 - 0.0385357BC \\ & + 0.000344296C^2 - 0.000175632ABC\end{aligned} \tag{S2}$$

Fig. S1a–c show the Pareto charts for each dye with the adsorbents POP1 and POP2, respectively. The factors are display from highest to lowest significance, where the columns that exceed the vertical line (significance line), indicate that are statistically significantly different from zero with a confidence level of 95%, given by the *P*-values of the ANOVA analysis. In the other hand, it expects the *P*-value to be less than the significance level (α = 0.05) or the absolute value of the *t*-ratio (critical) to be higher than 2.

In the Pareto chart of the calculated effects for POP1 it can be seen for the dyes Reactive blue 21 and Reactive yellow 145, all factors and interactions were not significantly influencing the response, except the pH, while for the Reactive red 250 the *CA* interaction was the only one statistically significant. Additionally, for this same dye, all the factors and interactions were positive, exclude the *AB* interaction. Moreover, for the Reactive yellow 145 the unique indirect factor was the pH. Finally, the amount of adsorbent and the *BC* interaction were the direct factors with the Reactive blue 21.

In the case of the POP2 (Fig. S2a–c), for the Reactive red 250 the unique statistically non-significant factors and interactions were pH and the *AB* and *ABC* interactions. Furthermore, the factor amount of adsorbent and the *AB* interaction are positive, that is, an increase in these variables causes an increase in the removal rate. In Reactive blue 21, the *AB* interaction and the adsorbent quantity factor were not statistically significant. In addition, this latest factor was the only that had a direct effect. With the dye Reactive yellow 145 the *AC*, *AB* and *BC* interactions did not have a statistically significant effect on the dye removal percentage, in addition, the *C* factor and the *ABC* and *AB* interactions had a direct effect.

S3.1. Effect of process variables on the percentage of dye removal

Fig. S3a and b show the removal profile of the dyes Reactive red 250, Reactive blue 21 and Reactive yellow 141, respectively, as a function of pH, treatment temperatures and amounts of biochar for POP1. Similarly, the Fig. S4a and b display the removal percentage of the same dyes as a function of the same parameters for POP2. It can observe that the removal performance for both bioadsorbents of all dyes increases along with the decrease in pH solution. In the specific case of POP2 the Reactive red 250, Reactive blue 21 and Reactive yellow 145 concentration decrease from 95.5% to 72.5%, 95.0% to 58.5% and 71.8% to 55.4%

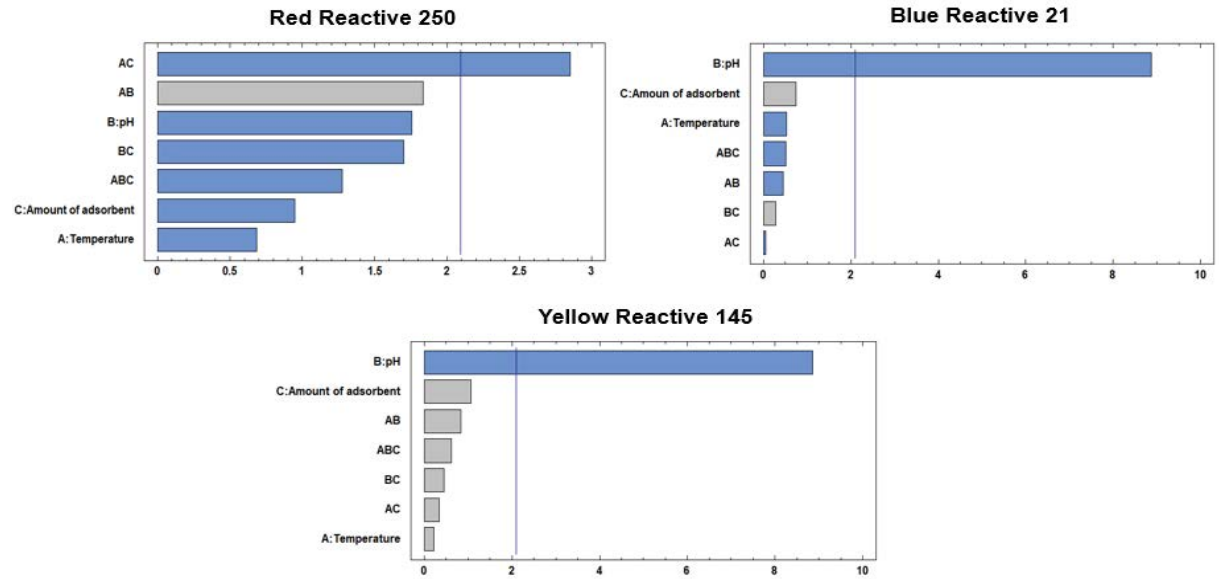

Fig. S1. Pareto chart of the calculated effects for POP1. Direct effects ▭, Indirect effects ▬.

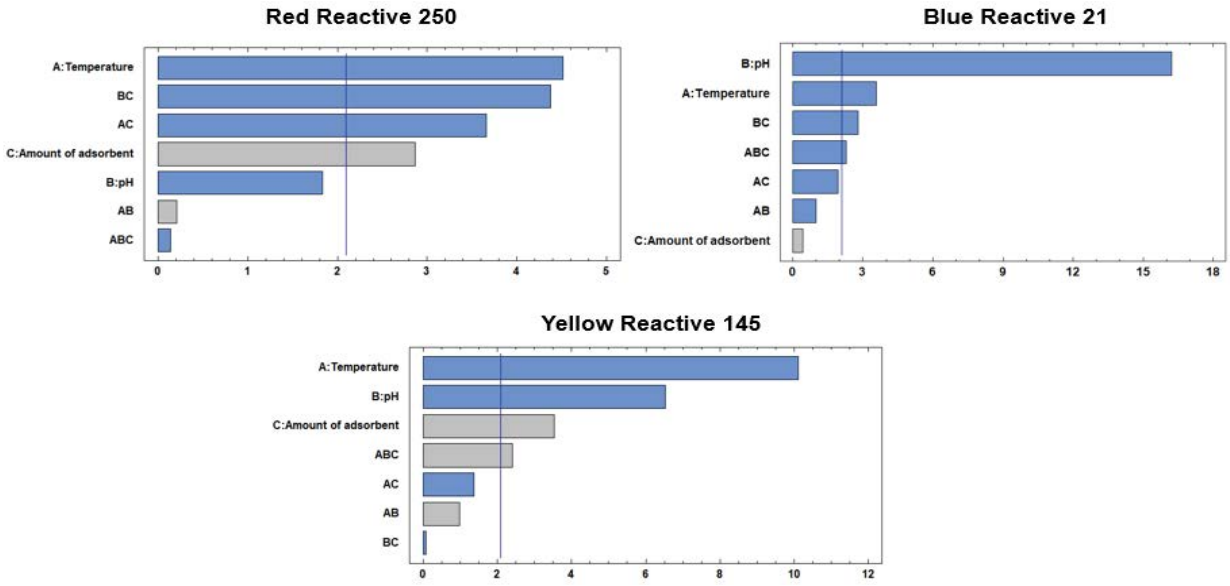

Fig. S2. Pareto chart of the calculated effects for POP2. Direct effects ▭, Indirect effects ▬.

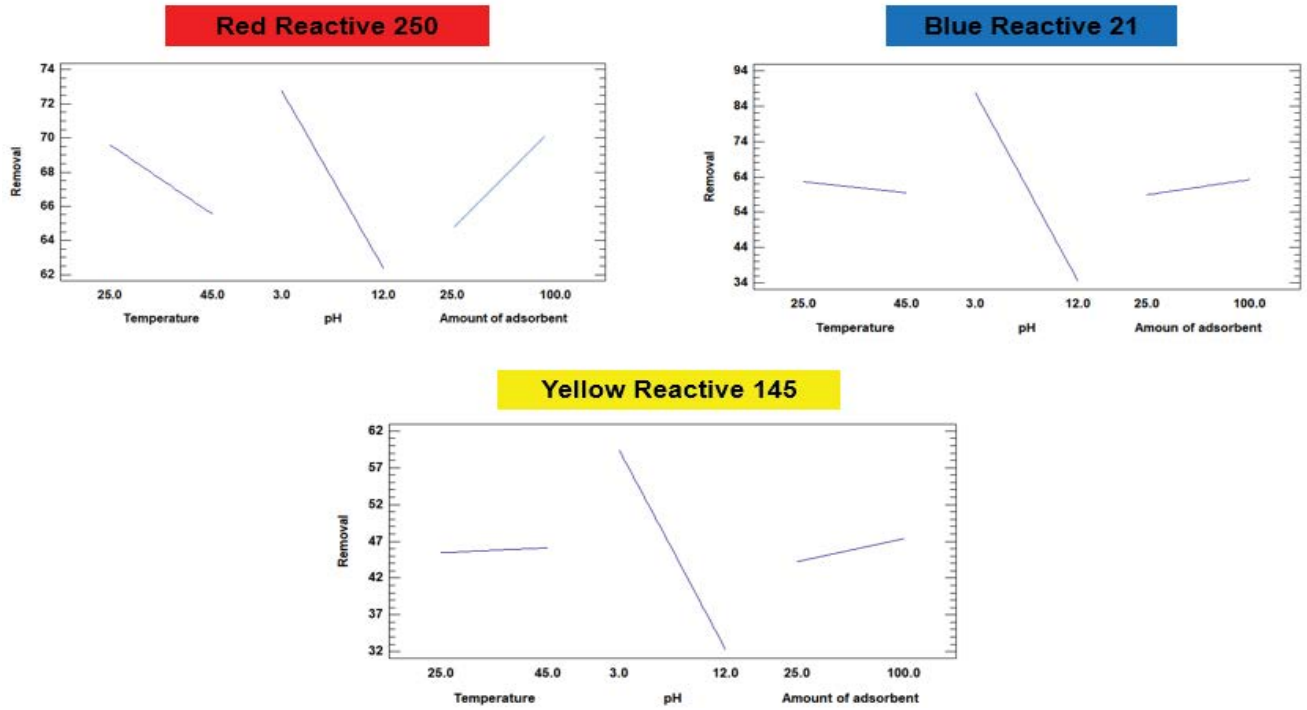

Fig. S3. Effect of pH, temperature and amount of bioadsorbent on the removal percentage of dyes from synthetical wastewater by POP1.

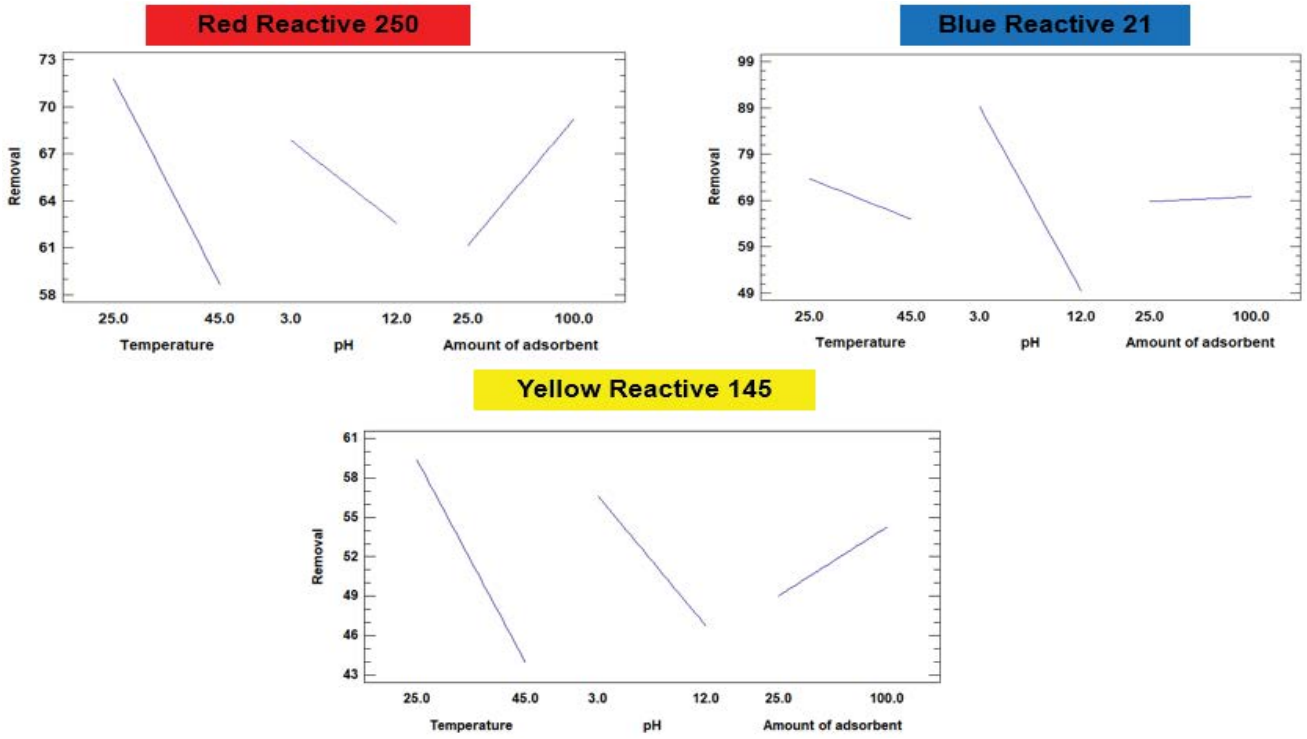

Fig. S4. Effect of pH, temperature and amount of bioadsorbent on the removal percentage of dye from synthetical wastewater by POP1.

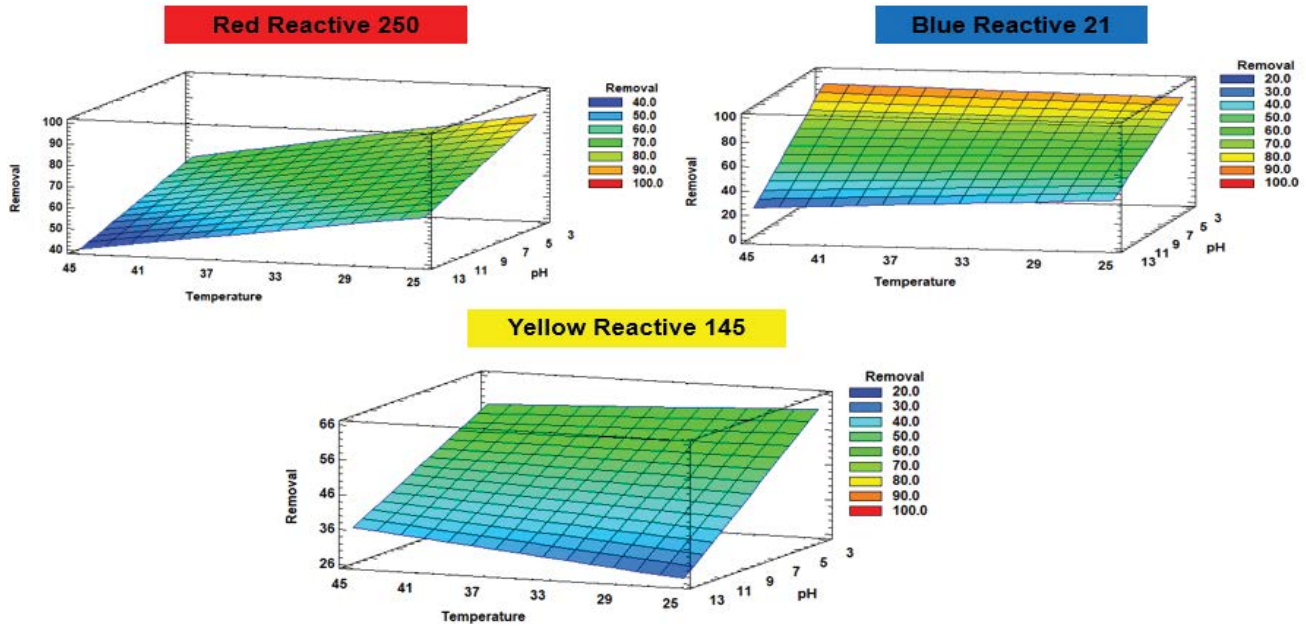

Fig. S5. Response surfaces for the effects of interaction between pH and temperature on the removal percentage of each dye with POP1.

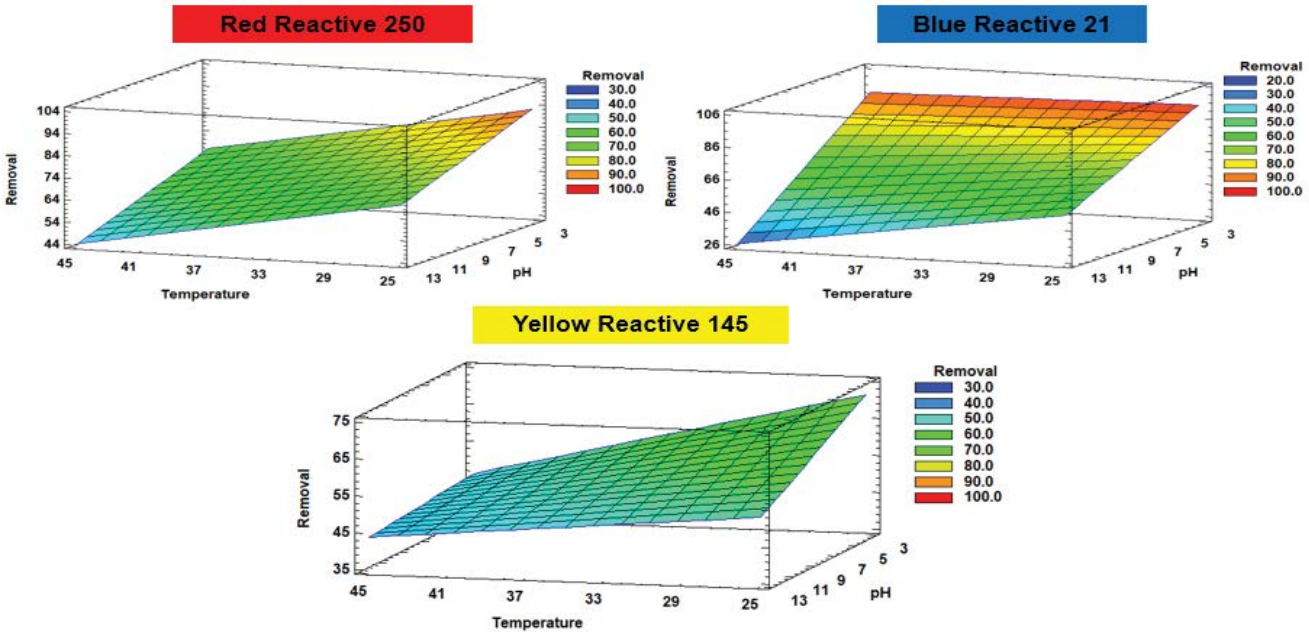

Fig. S6. Response surfaces for the effects of interaction between pH and temperature on the removal percentage of each dye with POP2.

respectively, when pH increases from pH 3.0 to pH 12.0. At the same time, POP1 showed a similar behavior to the adsorbent POP2 with the difference of lower removal percentages. According to the value reported for the isoelectric point of the bioadsorbents (4.5 and 4.8 for POP1 and POP2, respectively), it can be inferred that at pH < pH_{PZC} (zero point of charge) the surface of the materials will be positively charged, favoring the interaction with anionic species at acidic pH, which could explain the reason for the increase in removal (%) with decreasing pH.

Moreover, in the same figures it can be elucidated that with decrease in solution temperature, the dye removal percentages increase for both POP1 and POP2 biochars. On the other hand, the increase in removal (%) of all the dyes with decreasing temperature indicates that the adsorption process is exothermic.

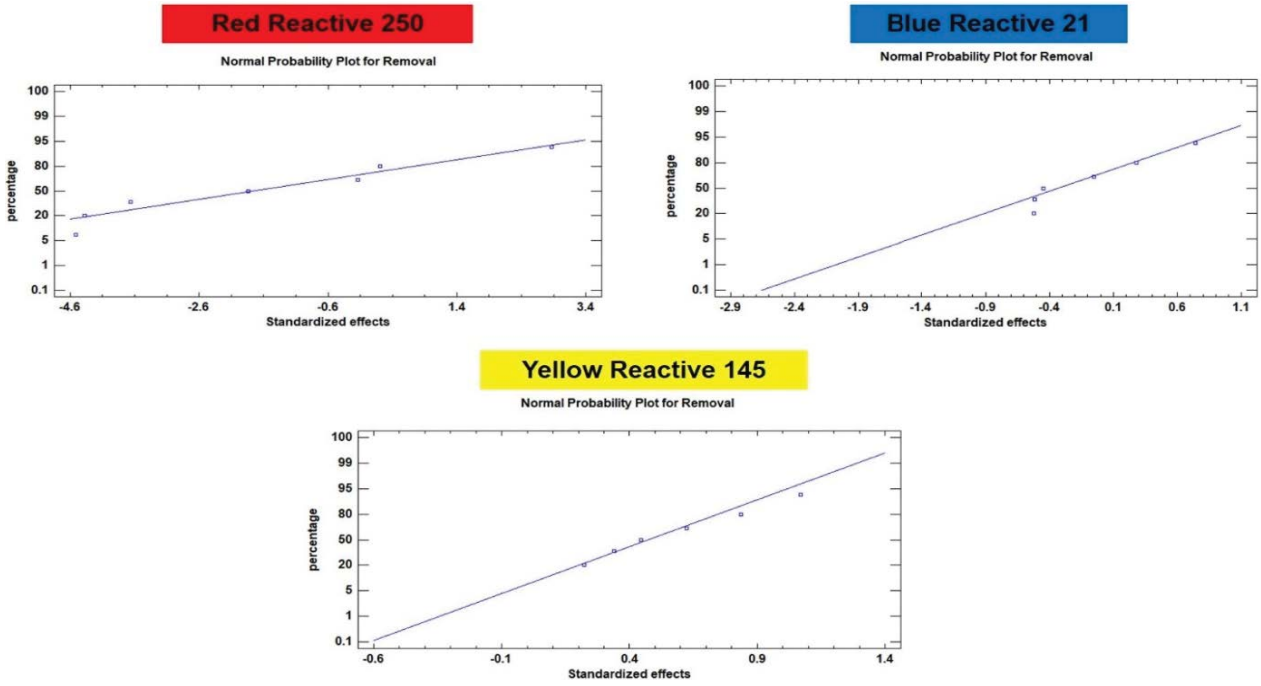

Fig. S7. Comparisons between experimental and predicted values with POP1.

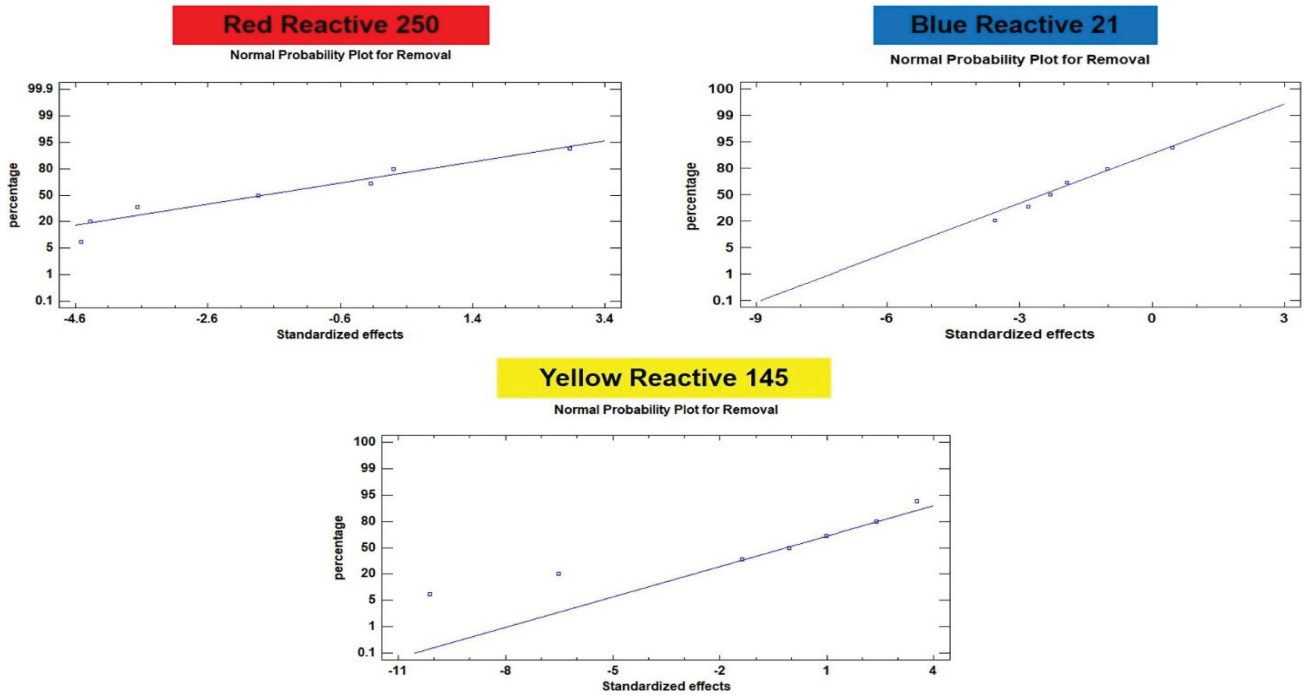

Fig. S8. Comparisons between experimental and predicted values with POP2.

Furthermore, it has been noticed that the dye removal percentages also increased with adsorbent dose increases for both biochars, for instance, for the POP2 the removal percentage of Reactive red 250, Reactive blue 21 and Reactive yellow 145 increases from 25 to 100 mg from 62.0% to 71.0%, 61.0% to 63.0% and 51.0% to 57.0%, respectively, this attributed to the increase removal (%) is because of the available sorption surface and availability of more adsorption sites.

The maximum removal percentage for reagents Reactive red 250, Reactive yellow 145 and Reactive blue 145 using POP1 were 90%, 66% and 99%, while, for the adsorbent

POP2, the removal percentages reached were 96% (Reactive red 250), 72% (Reactive yellow 145) and 95% (Reactive blue 145). The greatest desorption efficiency was obtained for the highest levels of the three factors (15 mL of desorbing solution, pH 10 and 200 rpm).

S3.2. Optimization of design parameters 3^3

The response surfaces for the interactions of different pairs of statistically significant factors on the dye removal efficiency for POP1 and POP2 are expressed in Figs. S5a & c and S6a–c, respectively. The optimum bioadsorbent dosage was found to be 100 mg for the removal of all dyes from synthetic wastewater, thus, 100 mg was fixed as an optimum dose for further adsorption experimental studies at pH and temperature values different. In summary, the highest dye removal percentage for all dyes and bioadsorbents were archive at 25°C, a pH of 3.0 and 100 mg of material.

As is gathered in Fig. S7a–c and S8a–c, the values of predicted removal percentage vs. experimental value were distributed close to the diagonal line, which means that the predictions of the empirical model correlate well with the observed results for both adsorbents, indicating that the model provides a good fit.